

# Ankyrin-G palmitoylation and $\beta$ II-spectrin binding to phosphoinositide lipids drive lateral membrane assembly

Meng He,<sup>1</sup> Khadar M. Abdi,<sup>2</sup> and Vann Bennett<sup>3,4,5</sup>

<sup>1</sup>Department of Pharmacology and Cancer Biology, <sup>2</sup>Department of Cell Biology, <sup>3</sup>Department of Biochemistry, and <sup>4</sup>Department of Neurobiology, Duke University Medical Center, Durham, NC 27710

<sup>5</sup>Howard Hughes Medical Institute, Durham, NC 27710

**A**nkyrin-G and  $\beta$ II-spectrin colocalize at sites of cell-cell contact in columnar epithelial cells and promote lateral membrane assembly. This study identifies two critical inputs from lipids that together provide a rationale for how ankyrin-G and  $\beta$ II-spectrin selectively localize to Madin-Darby canine kidney (MDCK) cell lateral membranes. We identify aspartate-histidine-histidine-cysteine 5/8 (DHHC5/8) as ankyrin-G palmitoyltransferases required for ankyrin-G lateral membrane localization and for assembly of lateral membranes. We also find that  $\beta$ II-spectrin functions as a coincidence detector that requires recognition of both ankyrin-G and phosphoinositide lipids

for its lateral membrane localization. DHHC5/8 and  $\beta$ II-spectrin colocalize with ankyrin-G in micrometer-scale subdomains within the lateral membrane that are likely sites for palmitoylation of ankyrin-G. Loss of either DHHC5/8 or ankyrin-G- $\beta$ II-spectrin interaction or  $\beta$ II-spectrin-phosphoinositide recognition through its pleckstrin homology domain all result in failure to build the lateral membrane. In summary, we identify a functional network connecting palmitoyltransferases DHHC5/8 with ankyrin-G, ankyrin-G with  $\beta$ II-spectrin, and  $\beta$ II-spectrin with phosphoinositides that is required for the columnar morphology of MDCK epithelial cells.

## Introduction

Spectrin and ankyrin are associated with the cytoplasmic surface of the plasma membrane where they cooperate in micrometer-scale organization of membrane-spanning proteins within specialized membrane domains in many vertebrate tissues (Bennett and Healy, 2009; Bennett and Lorenzo, 2013). A common organizational principle shared by spectrin/ankyrin-based domains, as presented in reviews and cartoons, is straightforward: membrane-spanning proteins, including cell adhesion proteins capable of responding to extracellular cues as well as membrane transporters, are “anchored” within the fluid bilayer by association with ankyrin, which in turn is coupled to an extended spectrin-actin network that is tightly associated with the plasma membrane (Bennett and Healy, 2009; Bennett and Lorenzo, 2013). However, these protein-based models, although descriptive of steady-state protein composition, do not provide an explanation for how membrane domains are actually assembled and precisely localized in cells.

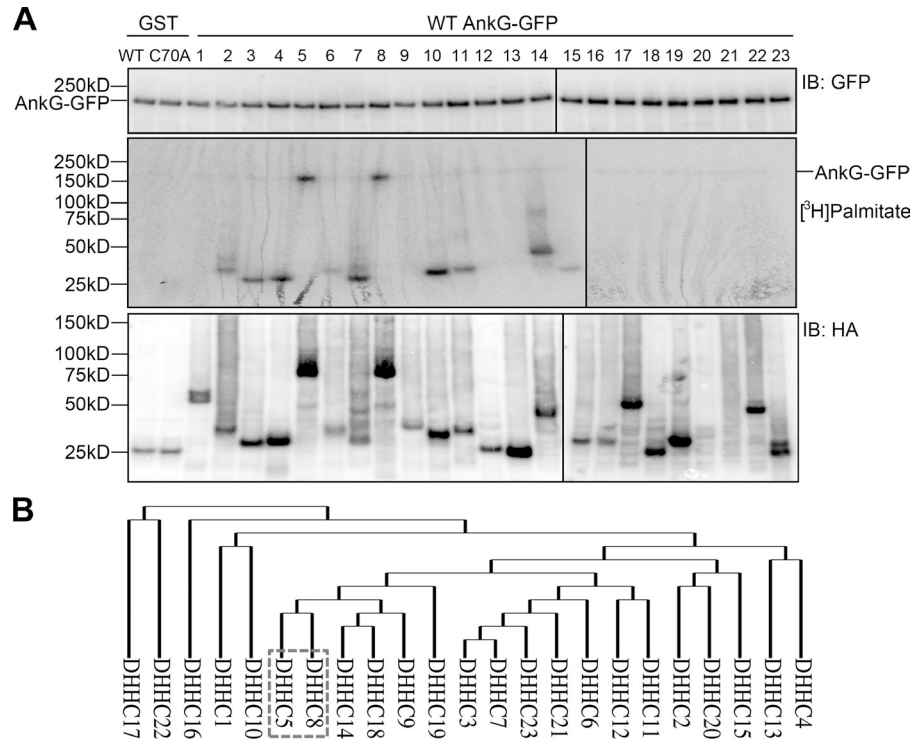
Membrane lipids and lipid modifications play important roles in determining plasma membrane identity. For example, phosphoinositide lipids are increasingly recognized as critical determinants of plasma membrane organization in addition to their roles in intracellular organelles (Martin-Belmonte et al., 2007; Shewan et al., 2011; Hammond et al., 2012; Johnson et al., 2012; Nakatsu et al., 2012). In addition, the aspartate-histidine-histidine-cysteine (DHHC) family of 23 protein palmitoyltransferases, first discovered in yeast, now are known to function in vertebrates in targeting and trafficking of membrane proteins (Bartels et al., 1999; Roth et al., 2002; Fukata et al., 2004; Fukata and Fukata, 2010; Greaves and Chamberlain, 2011).  $\beta$ -Spectrins contain a pleckstrin homology (PH) domain with preference for phosphatidylinositol 4,5-bisphosphate (PI(4,5)P<sub>2</sub>; Travé et al., 1995; Das et al., 2008). Moreover, ankyrin-G is S-palmitoylated at a conserved cysteine (C70; He et al., 2012). This palmitoylated

Correspondence to Vann Bennett: vann.bennett@duke.edu

Abbreviations used in this paper: ANOVA, analysis of variance; DHHC, aspartate-histidine-histidine-cysteine; PH, pleckstrin homology; PI(4,5)P<sub>2</sub>, phosphatidylinositol 4,5-bisphosphate; WT, wild type.

© 2014 He et al. This article is distributed under the terms of an Attribution-Noncommercial-Share Alike-No Mirror Sites license for the first six months after the publication date (see <http://www.rupress.org/terms>). After six months it is available under a Creative Commons license [Attribution-Noncommercial-Share Alike 3.0 Unported license, as described at <http://creativecommons.org/licenses/by-nc-sa/3.0/>].

**Figure 1. Ankyrin-G is palmitoylated by palmitoyltransferases DHHC5 and -8.** (A) Ankyrin-G-GFP was cotransfected into HEK293 cells with each of the 23 HA-DHHC. After metabolic labeling with [<sup>3</sup>H]palmitic acid, cells were lysed and analyzed by SDS-PAGE. (top) The expression level of ankyrin-G-GFP probed by  $\alpha$ -GFP antibody; (middle) autoradiograph showing the extent of protein labeling in cell extracts; (bottom) the expression level of the cotransfected HA-DHHC probed by  $\alpha$ -HA antibody. (B) The phylogenetic tree of the 23 mouse DHHC shows that DHHC5 and -8 are closely related.



cysteine is required for function of ankyrin-G in promoting formation of the lateral membrane of MDCK epithelial cells as well as assembly of axon initial segments in neurons (He et al., 2012). Together, these considerations suggest the membrane lipid environment and in particular phosphoinositides and protein palmitoylation are likely to work in concert with ankyrin- and spectrin-based protein interactions in establishing and/or regulating membrane domains.

Ankyrin-G and  $\beta$ II-spectrin localize at the lateral membranes of columnar epithelial cells where deficiency of either protein results in reduced cell height as well as impaired reassembly of new lateral membrane after cytokinesis (Kizhatil and Bennett, 2004; Kizhatil et al., 2007a; Jenkins et al., 2013). Ankyrin-G, in contrast to other lateral membrane-associated proteins, including its partners  $\beta$ II-spectrin and E-cadherin, persists on the plasma membrane of depolarized MDCK cells exposed to low calcium (He et al., 2012). Ankyrin-G thus is a candidate to function as a template for the rapid restoration of the lateral membrane that occurs after readdition of calcium. Ankyrin-G retention on the plasma membrane of depolarized MDCK cells, as well as its function in maintaining lateral membrane height, both require a conserved cysteine residue that is S-palmitoylated (He et al., 2012). These findings raise questions regarding the roles of palmitoyltransferases in directing polarized localization of ankyrin-G and  $\beta$ II-spectrin, as well as the functional hierarchy among these proteins in lateral membrane assembly.

The present study identifies DHHC5 and 8 as the only DHHC family members localized to the lateral membrane of MDCK cells and the two palmitoyltransferases responsible for palmitoylation and targeting of ankyrin-G. We also find that  $\beta$ II-spectrin requires binding to both ankyrin-G as well as PI(3,4)P<sub>2</sub>

and PI(3,4,5)P<sub>3</sub> phosphoinositide lipids to localize and function at lateral membranes.  $\beta$ II-Spectrin thus operates as a coincidence detector that ensures high spatial fidelity in its polarized targeting to the lateral membrane. Together these findings demonstrate a critical requirement of palmitoylation and phosphoinositide recognition in addition to protein-protein interactions for precise assembly of ankyrin-G and  $\beta$ II-spectrin at the lateral membrane of epithelial cells.

## Results

### DHHC5 and -8 are the physiological ankyrin-G palmitoyltransferases in MDCK cells

We previously demonstrated that cysteine 70 of ankyrin-G is palmitoylated and is required for ankyrin-G function in formation of lateral membranes of MDCK cells and axon initial segments of hippocampal neurons (He et al., 2012). We next sought to identify the palmitoyltransferases responsible for modifying ankyrin-G. A screening assay using metabolic labeling with [<sup>3</sup>H]palmitate in cells cotransfected with substrate and an individual member of the DHHC palmitoyltransferases has been widely used to determine enzyme specificity (Fukata et al., 2004, 2006; Fernández-Hernando et al., 2006; Iwanaga et al., 2009; Tsutsumi et al., 2009). Using this assay in HEK293T cells, we observed a dramatic increase of palmitoylation of ankyrin-G-GFP when coexpressed with either DHHC5 or 8, but not with the other 21 DHHC family members (Fig. 1 A).

A phylogenetic comparison of the 23 mouse DHHC proteins shows that DHHC5 and -8 are closely related (Fig. 1 B). DHHC5 and -8 use GRIP1b as a substrate in neurons and play critical roles in regulating AMPA-R trafficking (Thomas et al.,

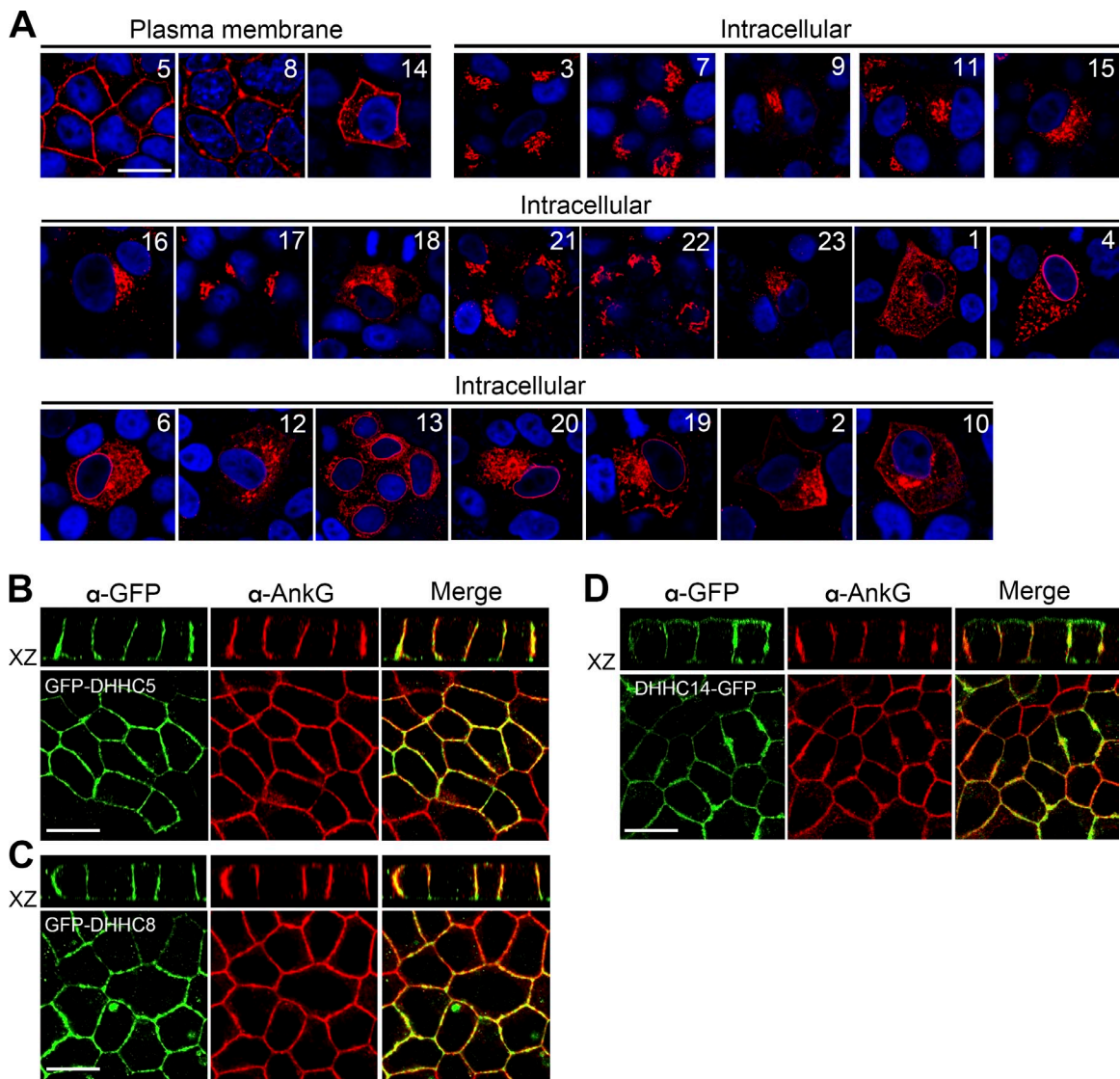


**Figure 2. DHHC5 and -8 colocalize with ankyrin-G at lateral membranes of MDCK cells.** (A) HA-DHHC 1–23 were expressed in MDCK cells and visualized by immunofluorescence (red,  $\alpha$ -HA; blue, DAPI). HA-DHHC5, 8, and 14 primarily localize to the plasma membrane, whereas the others exist in intracellular compartments. (B–D) GFP-tagged DHHC5, 8, or 14 were transfected into MDCK cells (green,  $\alpha$ -GFP; red,  $\alpha$ -ankyrin-G), and the XZ planes were reconstructed from confocal Z-stacks. Bars, 10  $\mu$ m.

2012). Additionally, DHHC5 also directly palmitoylates flotillin-2 and is required for flotillin-2 oligomerization (Li et al., 2012). However, no study has characterized the biological functions of DHHC5 and -8 palmitoyltransferases in epithelial cells.

We next asked where DHHC5 and -8 are localized in MDCK cells, and whether these particular palmitoyltransferases exhibit a distinct pattern compared with the other 21 DHHC family members. Tagged DHHC proteins exhibit specific localization patterns in nonpolarized HEK293T cells (Ohno et al., 2006). However, the localization of DHHC proteins in epithelial cells has not been reported. 20 of the HA-DHHC constructs transfected into MDCK cells localized to intracellular compartments, most likely the Golgi–ER network as previously described (Ohno et al., 2006). However, DHHC5, 8, and 14 predominantly localized to the plasma membrane when viewed in XY sections (Fig. 2 A). The plasma membrane localization of DHHC8 and 14 in MDCK cells was unexpected because these

proteins are primarily intracellular in HEK293T cells (Ohno et al., 2006). 3D confocal imaging in MDCK cells revealed that DHHC5 and -8 are polarized and confined to the lateral membrane together with ankyrin-G (Fig. 2, B and C). DHHC14, in contrast to DHHC5 and -8, localizes equally to both lateral and apical membranes (Fig. 2 D). DHHC5 and -8 thus are the only family members that colocalize with ankyrin-G on the lateral membranes of MDCK cells.

We next asked whether DHHC5 and -8 were required for ankyrin-G palmitoylation in MDCK cells. We first confirmed that both DHHC5 and -8 are natively transcribed in cultured MDCK cells using RT-PCR (Fig. 3 A). Then we developed a cell-sorting strategy for generating doxycycline-inducible shRNA stable cell lines to study effects of knockdown of DHHC5 and -8, either separately or together. We modified the single lentiviral vector Tet-inducible shRNA system (pLKO-Tet-On; Wiederschain et al., 2009) in two ways: (1) the puromycin resistance gene was

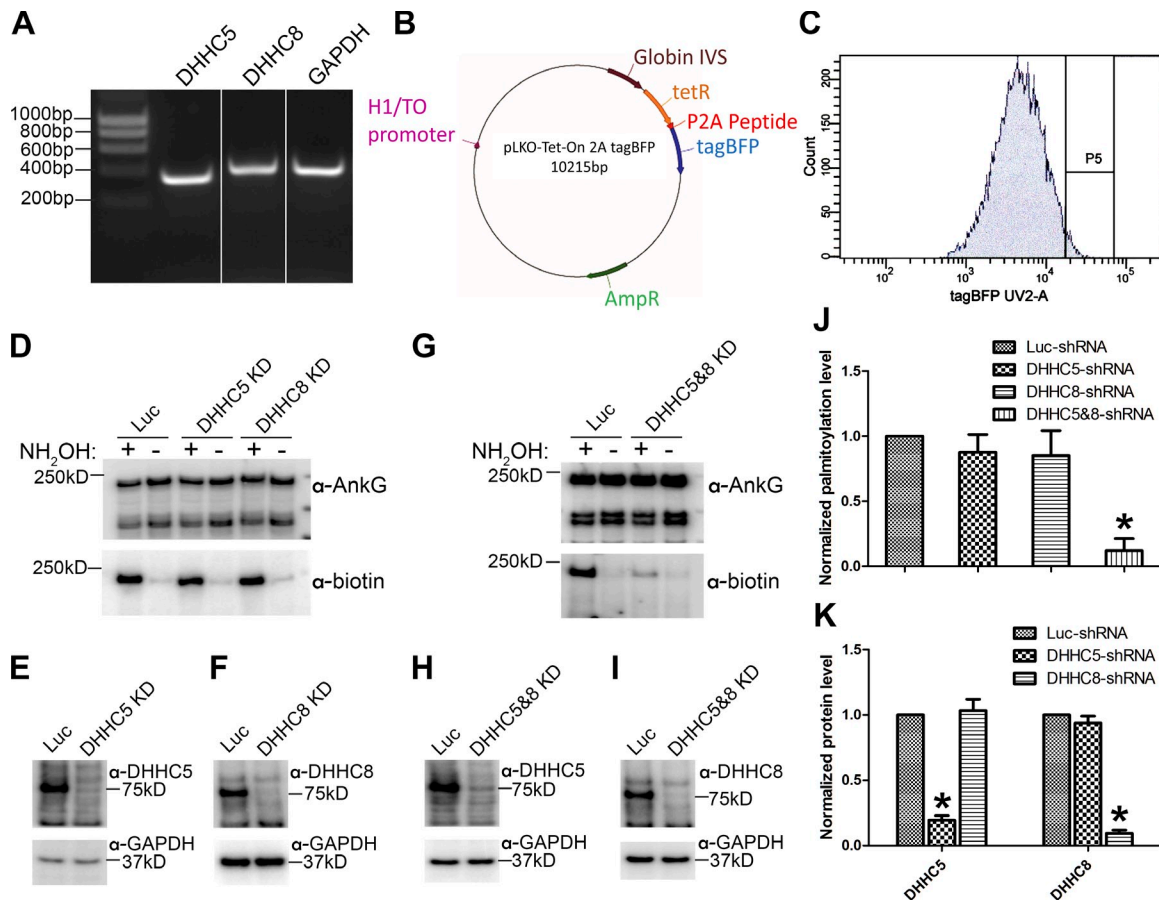


**Figure 3. DHH5 and -8 exhibit functional redundancy in palmitoylation of ankyrin-G.** (A) The RT-PCR shows that DHH5 and -8 are natively transcribed in MDCK cells. (B and C) The cell sorting strategy for making inducible shRNA cell lines. P5 indicates the collected cell population (~1%). (D–F) Single knockdown of DHH5 or 8 shows no reduction of ankyrin-G palmitoylation. Endogenous ankyrin-G was immunoprecipitated and analyzed using acyl biotin exchange assay (D) or the silencing efficiency of DHH5 (E) or 8 (F). (G–I) Double knockdown of DHH5 and -8 causes significant reduction of ankyrin-G palmitoylation. (J) Quantification of the normalized ankyrin-G palmitoylation level; mean  $\pm$  SEM. Results were analyzed using one-way ANOVA and Tukey's tests; \*,  $P < 0.001$ ;  $n = 3–5$ . (K) Quantification of DHH5 and DHH8 protein levels in Luc-, DHH5-, and DHH8-shRNA stable cell lines. Results were analyzed using one-way ANOVA and Tukey's tests; \*,  $P < 0.001$ ;  $n = 3$ .

replaced with DNA encoding the fluorescent protein TagBFP (excite 402; emit 457) to allow fluorescent cell sorting without interfering with other fluorescent tags such as GFP or mCherry; (2) the internal ribosome entry site was replaced with a 2A “self-splicing” peptide linker to ensure that stimulation of shRNA expression also efficiently stimulated expression of TagBFP (Fig. 3 B). Through cell sorting, we were able to select a small population of cells with similar levels of shRNA expression (Fig. 3 C).

DHH5 and -8 genes of *Canis lupus familiaris* share identical genomic sequences in multiple regions, which allow individual knockdown or selection of a single hairpin simultaneously targeting both genes in MDCK cells. An acyl-biotin exchange assay was used to assess ankyrin-G palmitoylation (Fig. S1 A; Drisdell et al., 2006). Single knockdown of either DHH5 or 8 had no effect on palmitoylation of ankyrin-G (Fig. 3, D, E, F, and J). We demonstrated this was not caused by up-regulation of one palmitoyltransferase after silencing the other one (Fig. S1 B and Fig. 3 K). However, silencing both DHH5 and -8 markedly reduced ankyrin-G palmitoylation (Fig. 3, G–J). In summary, DHH5 and -8 are the physiological palmitoyltransferases responsible for palmitoylating ankyrin-G

in MDCK cells based on their unique behavior compared with the other 21 DHH family members in palmitoylating ankyrin-G in heterologous cells, their colocalization with ankyrin-G at the lateral membranes of MDCK cells, as well as loss of ankyrin-G palmitoylation after their knockdown in MDCK cells.

#### DHH5/8 double knockdown phenocopies loss of ankyrin-G in MDCK cells

We next examined effects of knockdown of DHH5 and -8 on subcellular localization of endogenous ankyrin-G and on cell height. In the DHH5/8 double knockdown cells, ankyrin-G staining spread from the plasma membrane to the cytosol, in contrast to the single knockdown or control cells where ankyrin-G was confined to the lateral membrane (Fig. 4, A and D). Residual ankyrin-G staining on the lateral membrane may result from residual palmitoylation, which was only 90% complete, and/or interaction with E-cadherin and/or  $\beta$ II-spectrin. In addition, 110- and 120-kD cross-reacting polypeptides (Fig. 4 B) likely resulting from alternative splicing lack ANK repeats and are not subject to palmitoylation (Peters et al., 1995; Hoock et al., 1997; He et al., 2012). The loss of membrane staining was

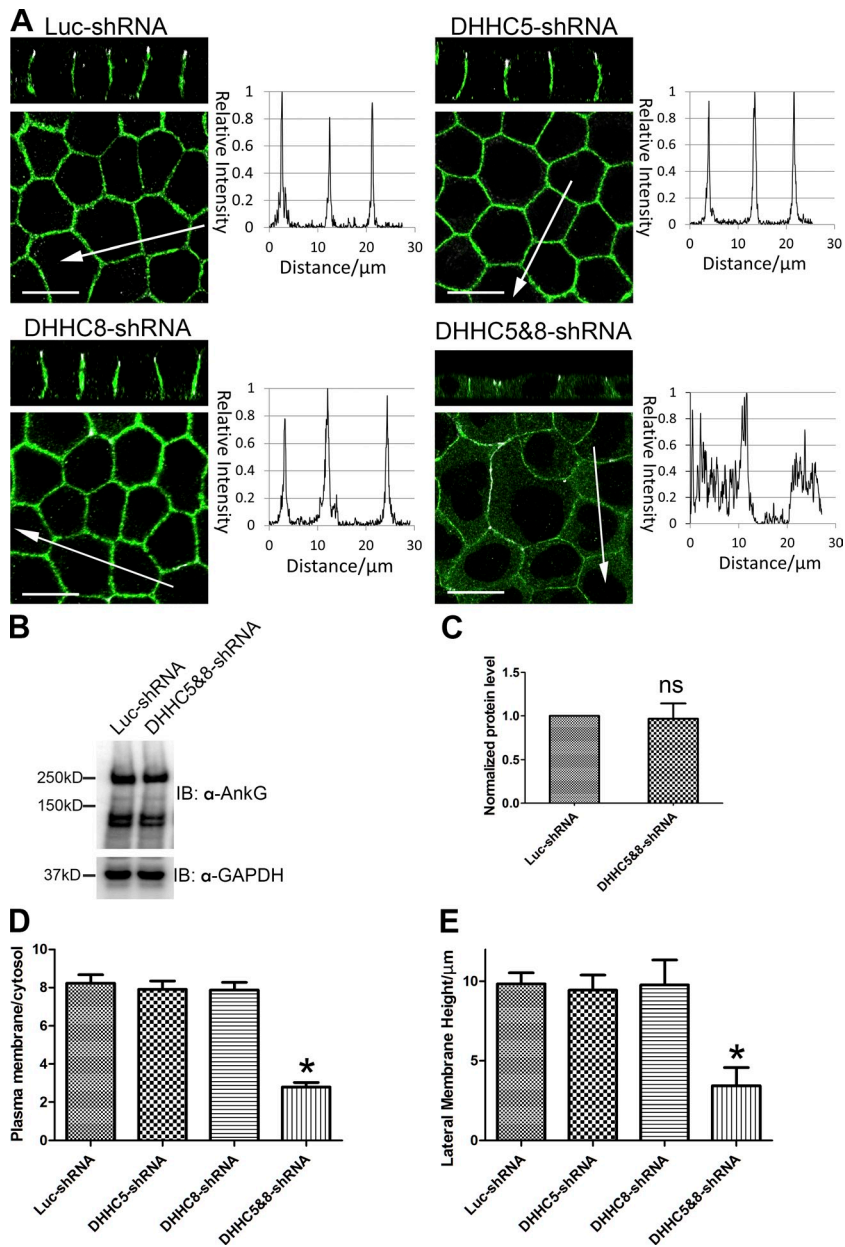


**Figure 4. Double knockdown of DHH5 and -8 in MDCK cells causes disassociation of ankyrin-G from the plasma membrane and reduces lateral membrane height.** (A) The inducible shRNA cell lines were treated with doxycycline to knockdown indicated genes, and then were fixed for immunofluorescence (green,  $\alpha$ -ankyrin-G; white,  $\alpha$ -ZO-1). The profiles represent the  $\alpha$ -ankyrin-G fluorescence intensities across the regions of interest indicated by the white arrows. Bars, 10  $\mu\text{m}$ . (B) Representative Western blot showing ankyrin-G levels after silencing DHH5 and -8. (C) Quantification of the normalized ankyrin-G level in DHH5/8-silenced cells; mean  $\pm$  SEM; student's *t* test; ns, not significant ( $P = 0.8$ );  $n = 4$ . (D) Quantification of the  $\alpha$ -ankyrin-G fluorescence intensity ratio of plasma membrane to cytosol. Results were analyzed using one-way ANOVA and Tukey's tests; \*,  $P < 0.001$ ;  $n = 47$ –53. (E) Quantification of the lateral membrane height. Results were analyzed using one-way ANOVA and Tukey's tests; \*,  $P < 0.001$ ;  $n = 47$ –53.

not caused by reduction of ankyrin-G expression level based on immunoblots of control and DHH5/8 double knockdown cells (Fig. 4, B and C). Interestingly, the DHH5/8 double knockdown cell monolayer exhibited a markedly reduced lateral membrane height (Fig. 4, A [the XZ plane] and E), thus phenocopying loss of ankyrin-G (Kizhatil and Bennett, 2004; Kizhatil et al., 2007b). This result is consistent with previous findings that ankyrin-G requires its palmitoylated cysteine 70 to restore the lateral membrane in ankyrin-G-depleted MDCK cells (He et al., 2012).

MDCK cells require millimolar concentrations of calcium to achieve apical-basolateral polarity and reversibly lose their polarity when transferred to a low calcium medium (Martinez-Palomo et al., 1980). We previously reported that ankyrin-G remains on the plasma membrane in unpolarized MDCK cells exposed to low calcium, whereas its binding partners E-cadherin

and  $\beta$ II-spectrin relocate to intracellular sites (Fig. 5 A; He et al., 2012). In contrast, C70A ankyrin-G mutant, which is resistant to palmitoylation, also exhibited loss of plasma membrane staining in unpolarized MDCK cells (He et al., 2012). Under the same low calcium condition, DHH5 and -8 remain localized to the plasma membrane together with ankyrin-G (Fig. 5 B). Moreover, double knockdown of DHH5 and -8 abolished the plasma membrane localization of ankyrin-G in unpolarized MDCK cells (Fig. 5 C and Fig. S1 E). These results together with loss of membrane association by the C70A ankyrin-G mutant demonstrate that palmitoylation of ankyrin-G by DHH5/8 drives its association with the plasma membrane in unpolarized MDCK cells.

We next compared effects of knockdown of either DHH5/8 or 210-kD ankyrin-G on lateral membrane reassembly after restoration of calcium. Control cells (Luc-shRNA) experienced

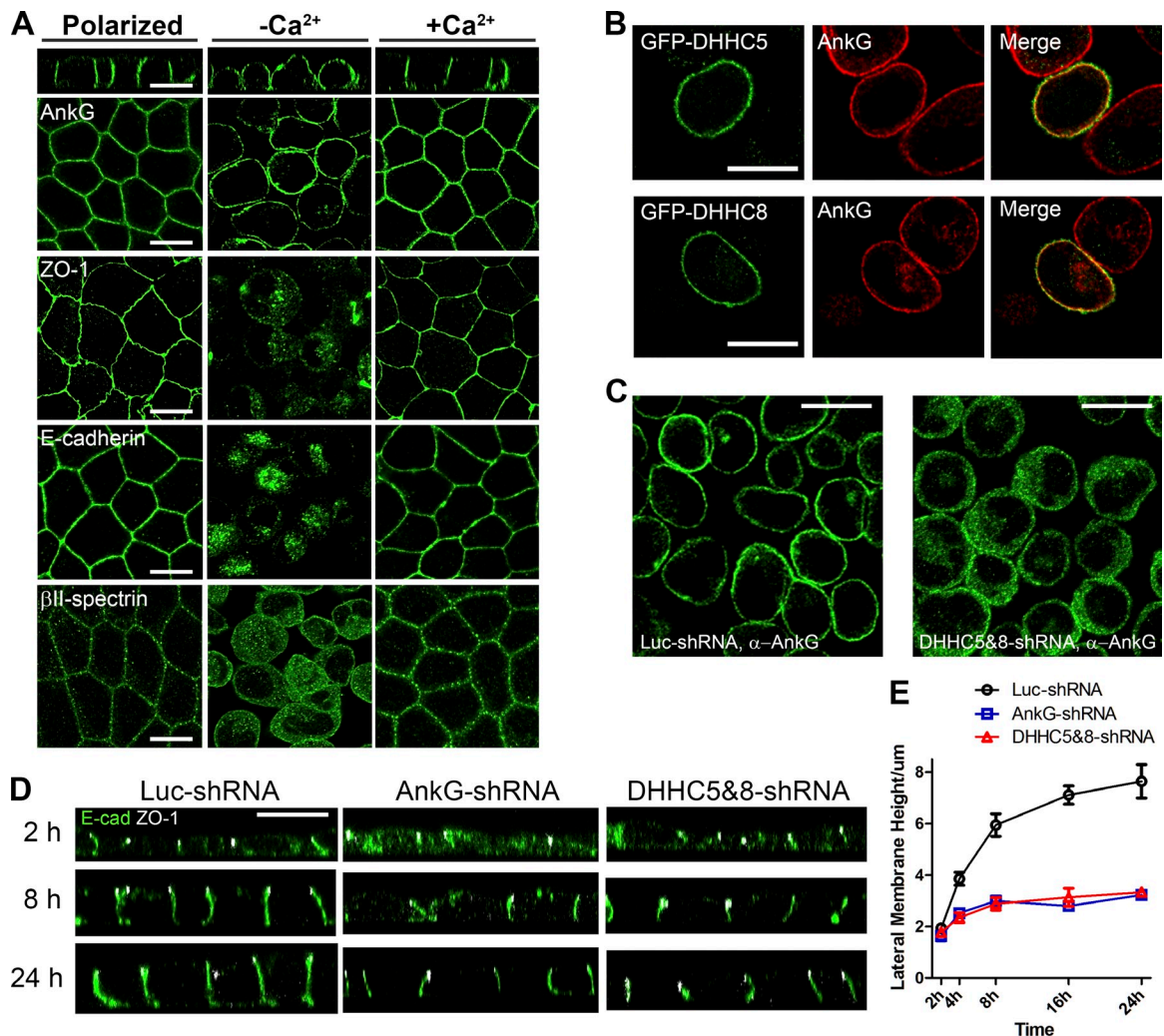


**Figure 5. DHHC5/8 and ankyrin-G are required for lateral membrane reassembly after calcium switch.** (A) Ankyrin-G persists on the plasma membrane in unpolarized MDCK cells. Polarized MDCK cells were trypsinized and grown in  $\text{Ca}^{2+}$ -depleted medium for 24 h before fixation ( $-\text{Ca}^{2+}$ ) or switched back to regular medium for another 24 h ( $+\text{Ca}^{2+}$ ). Samples were stained against ankyrin-G, ZO-1, E-cadherin, or  $\beta$ II-spectrin. (B) GFP-DHHC5 and -8 colocalize with ankyrin-G in unpolarized MDCK cells [green,  $\alpha$ -GFP; red,  $\alpha$ -ankyrin-G]. (C) DHHC5/8-silenced cells or control cells (Luc-shRNA) were plated in  $\text{Ca}^{2+}$ -depleted medium and fixed to stain against endogenous ankyrin-G. (D) DHHC5/8 or ankyrin-G-silenced cells fail to reassemble the lateral membrane after calcium switch. Stable shRNA cells were induced by to knockdown-indicated genes, and then plated in  $\text{Ca}^{2+}$ -depleted medium. 24 h later, cells were switched back to regular medium and fixed at different time points: 2, 4, 8, 16, and 24 h [green,  $\alpha$ -E-cadherin; white,  $\alpha$ -ZO-1]. Bars, 10  $\mu\text{m}$ . (E) Quantification of the lateral membrane heights; mean  $\pm$  SEM;  $n = 17$ –31.

rapid biosynthesis of the lateral membrane and grew from  $\sim 2$  to 8  $\mu\text{m}$  in height within 24 h. In contrast, cells depleted of either 210-kD ankyrin-G or DHHC5/8 failed to restore lateral membrane height and grew from 2 to only 3  $\mu\text{m}$  over the same period (Fig. 5, D and E; and Fig. 6 C for extent of 210-kD ankyrin-G knockdown). We also showed that during the repolarization process, there was no significant change of DHHC5 and -8 protein level (Fig. S1, C and D). However, loss of 210-kD ankyrin-G or DHHC5/8 did not affect the establishment of cell polarity, indicated by unaltered tight junction staining for ZO-1 and lateral membrane staining for E-cadherin (Fig. 5 D). Cells depleted of either ankyrin-G or DHHC5/8 still maintained a residual lateral membrane of  $\sim 3 \mu\text{m}$ . The remaining lateral membrane may result from incomplete knockdown as detectable levels of ankyrin-G as well as DHHC5/8 persist in shRNA-expressing

cells (Fig. 3, H and I; and Fig. 6 C). Alternatively, the residual height of 2–3  $\mu\text{m}$  may represent lateral membrane that is independent of the ankyrin-G–DHHC5/8 pathway.

#### **$\beta$ II-Spectrin requires both ankyrin-G and phosphoinositides for lateral membrane targeting**

Results so far demonstrate that palmitoylation of ankyrin-G by DHHC5/8 is required for targeting ankyrin-G to the lateral membrane as well as for reassembly of the lateral membrane after restoration of calcium to unpolarized MDCK cells. We next addressed the role of ankyrin-G in targeting  $\beta$ II-spectrin to the lateral membrane.  $\beta$ II-Spectrin potentially can associate with plasma membranes either through its ankyrin-binding site (Davis et al., 2009; Ipsaro et al., 2009) and/or through a PH

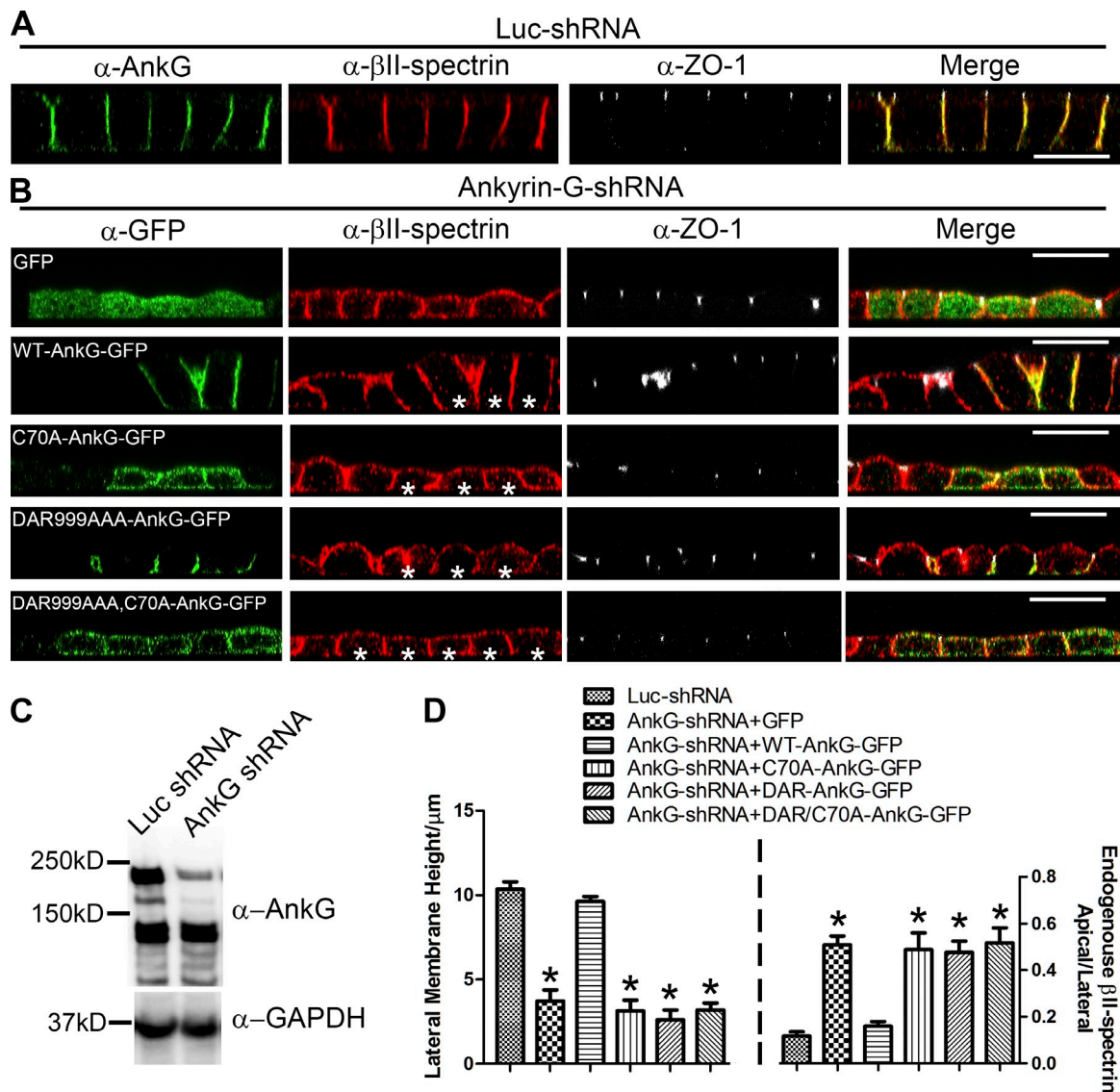
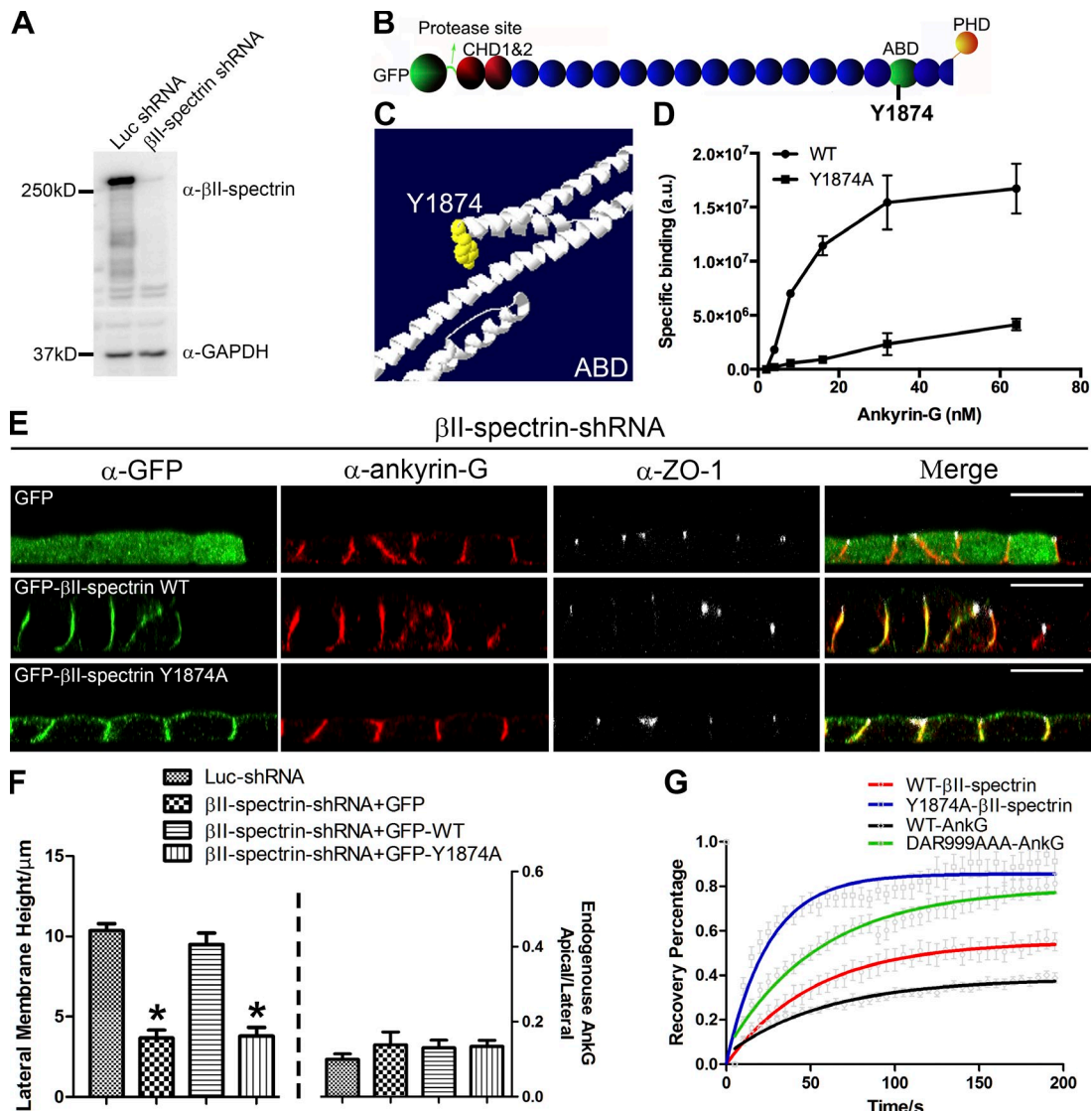


Figure 6. **Ankyrin-G determines the polarized recruitment of  $\beta$ II-spectrin to the lateral membrane.** (A) Immunostaining of endogenous proteins in Luc-shRNA control cells (green,  $\alpha$ -ankyrin-G; red,  $\alpha$ - $\beta$ II-spectrin; white,  $\alpha$ -ZO-1). (B) Ankyrin-G-shRNA cells were induced to knockdown endogenous ankyrin-G and transfected with GFP, WT-AnkG-GFP, C70A-AnkG-GFP, DAR999AAA-AnkG-GFP, or DAR999AAA/C70A-AnkG-GFP, and then fixed for immunostaining (green,  $\alpha$ -GFP; red,  $\alpha$ - $\beta$ II-spectrin; white,  $\alpha$ -ZO-1). Asterisks indicate transfected cells. Bars, 10  $\mu$ m. (C) The representative Western blot showing ankyrin-G knockdown efficiency. (D) Quantification of the height of lateral membranes and the apical mislocalization of endogenous  $\beta$ II-spectrin under each experimental condition. Results were analyzed using one-way ANOVA and Tukey's tests; \*,  $P < 0.001$ ; mean  $\pm$  SEM;  $n = 17$ –23.

domain that binds to phosphoinositide lipids (Hyvönen et al., 1995; Wang and Shaw, 1995; Wang et al., 1996; Das et al., 2006, 2008). Analysis of epistatic relationships between  $\beta$ -spectrin and the two ankyrin genes in *Drosophila melanogaster* indicate cell type-specific variations in use of PH domains and ankyrin-binding activities (Das et al., 2006, 2008; Garbe et al., 2007; Mazock et al., 2010). We therefore wanted to determine how  $\beta$ II-spectrin assembles on the lateral membrane in MDCK cells.

We first examined the effects of silencing ankyrin-G on the localization of endogenous  $\beta$ II-spectrin. In control cells, both ankyrin-G and  $\beta$ II-spectrin primarily localize to the lateral membrane (Fig. 6 A), which is consistent with previous findings (Kizhatil et al., 2007b). Interestingly, in the absence of ankyrin-G,  $\beta$ II-spectrin mislocalized to the apical membrane in MDCK cells (Fig. 6 B, top). We next addressed the contributions of

ankyrin-G binding and palmitoylation on  $\beta$ II-spectrin localization by evaluating mutation of ankyrin-G that abolishes its binding to  $\beta$ II-spectrin (DAR999AAA) or its palmitoylation (C70A). In each set of experiments, native 210-kD ankyrin-G was knocked down and replaced with either GFP-tagged wild-type (WT) or mutated proteins. We used the same approach of doxycycline-inducible knockdown as used with DHHC5 and -8 (see Materials and methods; Fig. 3) to achieve inducible loss of 80–90% of native 210-kD ankyrin-G (Fig. 6 C). Cells induced for shRNA expression were subsequently transfected within 24 h with GFP-tagged 190-kD ankyrin-G or  $\beta$ II-spectrin (see Materials and methods). 190-kD ankyrin-G and the native 210-kD ankyrin-G differ in that 210-kD ankyrin-G contains additional residues in the C-terminal regulatory domain (unpublished data). However, 190- and 210-kD ankyrin-G do not exhibit any difference



**Figure 7. Interaction between Ankyrin-G and βII-spectrin determines their dynamics on the plasma membrane but is dispensable for ankyrin-G targeting.** (A) The representative Western blot showing βII-spectrin knockdown efficiency. (B) The schematic diagram of GFP-βII-spectrin construct with precision protease site (CHD, calponin homology domain; ABD, ankyrin-binding domain; PHD, PH domain). (C) The atomic structure of βII-spectrin's ankyrin-binding domain; residue Y1874 is highlighted in yellow. (D) The protein binding curve of ankyrin-G with WT βII-spectrin or the Y1874A mutant;  $n = 2$ . (E) βII-spectrin-shRNA cells were induced to knockdown endogenous βII-spectrin and transfected with GFP, GFP-βII-spectrin WT, or GFP-βII-spectrin Y1874A, and then fixed for immunostaining (green, α-GFP; red, α-ankyrin-G; white, α-ZO-1). Bars, 10 μm. (F) Quantification of the height of lateral membranes and the apical mislocalization of endogenous ankyrin-G under each experimental condition. Results were analyzed using one-way ANOVA and Tukey's tests; \*,  $P < 0.001$ ; mean  $\pm$  SEM;  $n = 21$ – $27$ . (G) FRAP shows the dynamics of GFP-tagged WT βII-spectrin or the Y1874A mutant and GFP-tagged WT ankyrin-G or the DAR999AAA mutant on the lateral membrane ( $n = 6$ – $11$ ).

in localization or ability to restore the lateral membrane in MDCK cells (unpublished data).

GFP-tagged WT ankyrin-G rescued the lateral membrane, as well as the polarity of endogenous βII-spectrin (Fig. 6, B and D, WT). However, DAR999AAA mutation of ankyrin-G that abolishes its binding to spectrin (Kizhatil et al., 2007b; Ipsaro et al., 2009; Ipsaro and Mondragón, 2010) lost activity in restoring the lateral membrane in ankyrin-G-silenced cells (Kizhatil et al., 2007b) as well as polarity of endogenous βII-spectrin (Fig. 6, B and D, DAR999AAA). Interestingly, DAR999AAA ankyrin-G still maintained its polarized localization at the residual lateral membrane, presumably because of palmitoylation and/or interaction with E-cadherin (Fig. 6 B, DAR999AAA). Similarly, the

C70A mutation of ankyrin-G that abolishes its palmitoylation also failed to rescue the lateral membrane (He et al., 2012) and the polarity of βII-spectrin (Fig. 6, B and D, C70A). In DHHC5/8-shRNA cells, βII-spectrin also mislocalized to the apical membranes (Fig. S2 E), which is consistent with our hypothesis that palmitoylation of ankyrin-G plays a role in the polarity of βII-spectrin localization. The endogenous βII-spectrin persists on apical and lateral plasma membranes instead of relocating in the cytoplasm together with C70A ankyrin-G, which still maintains βII-spectrin binding activity (Fig. S2, A and B). We also found that the double mutant (DAR999AAA/C70A), which loses both palmitoylation and spectrin binding activity, behaved similarly to the C70A ankyrin-G (Fig. 6, B and D, DAR999AAA/C70A).

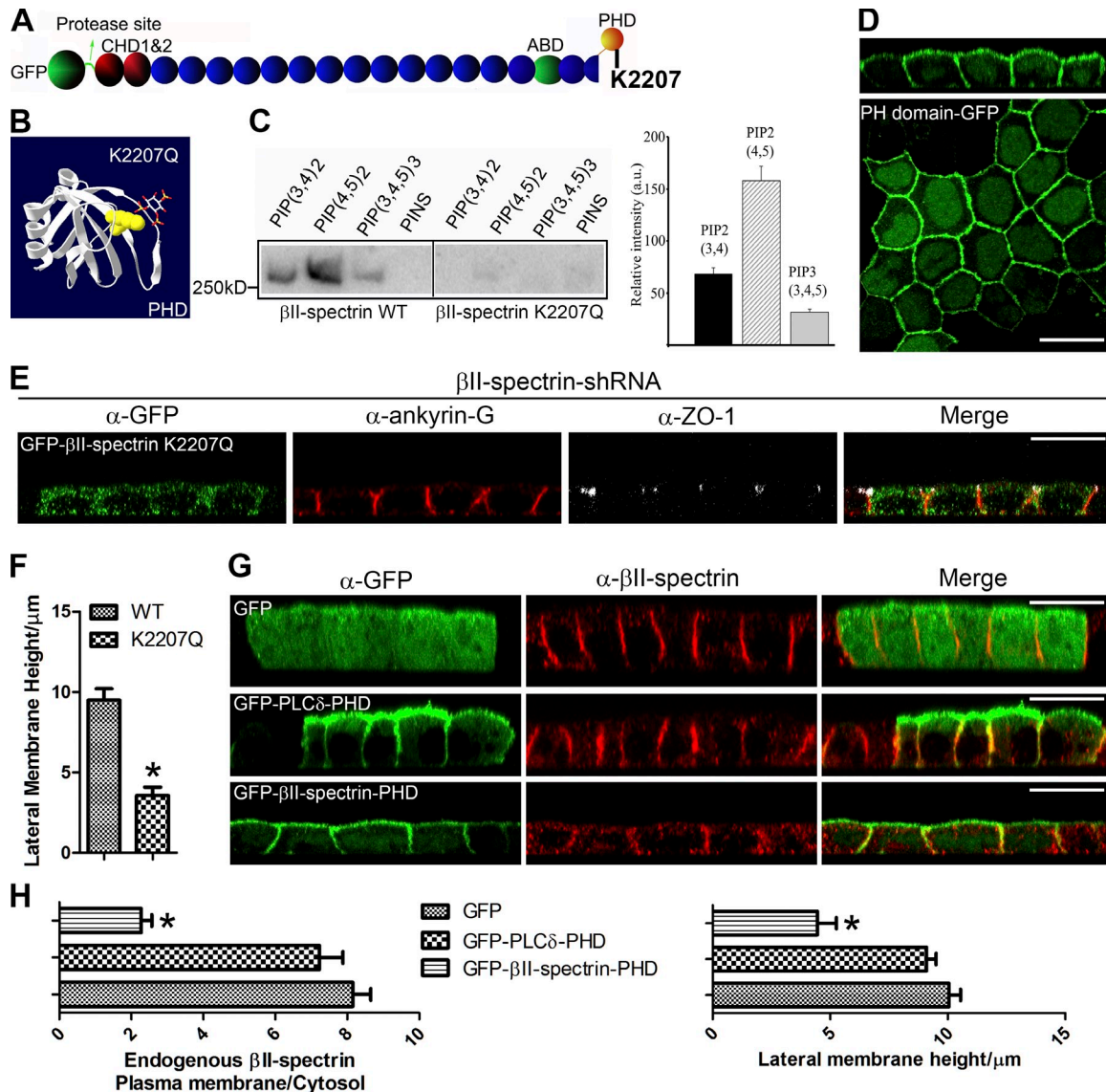
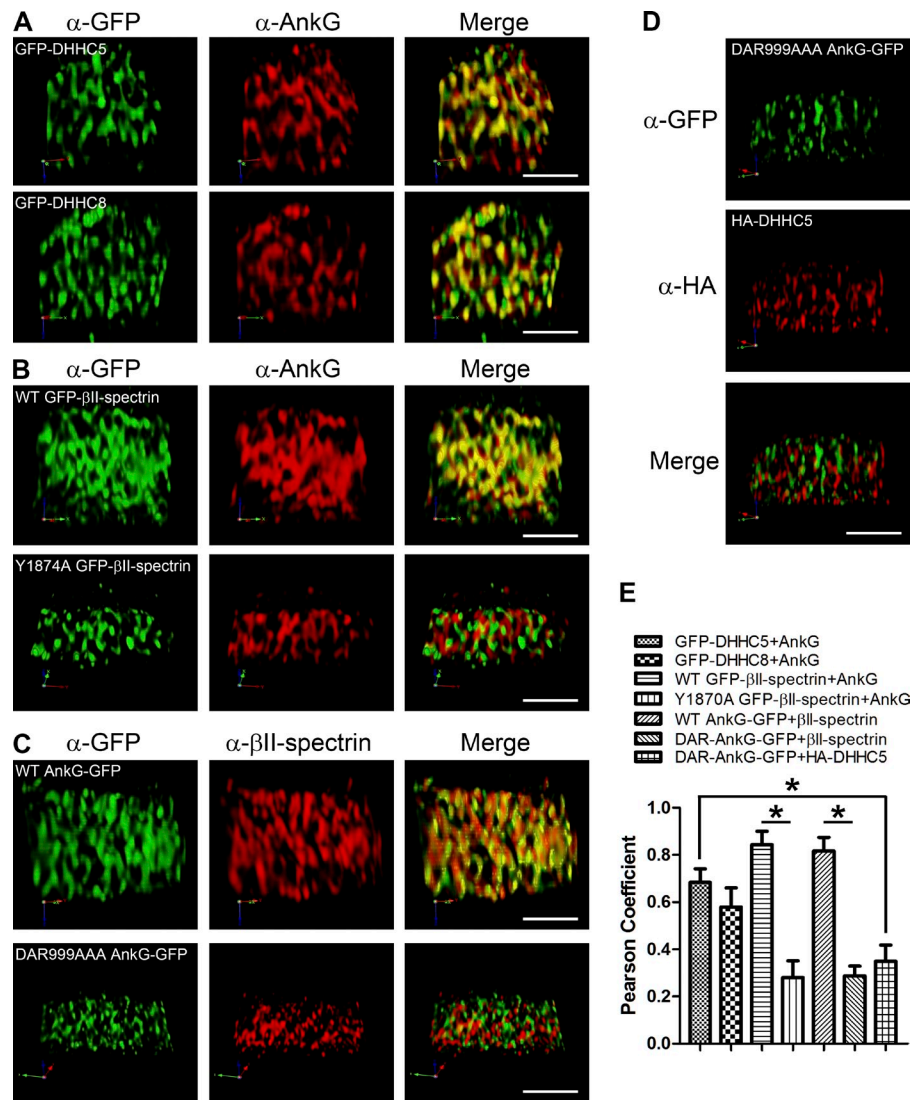


**Figure 8.  $\beta$ II-Spectrin targets to the plasma membrane through its PH domain by binding to multiple phosphoinositide lipids.** (A) The schematic diagram of K2207Q GFP- $\beta$ II-spectrin. (B) The atomic structure of the PH domain (PHD); the key residue required for phosphoinositide binding is highlighted in yellow. (C) The blots and quantification show the binding affinity of WT  $\beta$ II-spectrin or K2207Q mutant to different phosphatidylinositol-labeled liposomes (PI(3,4)P<sub>2</sub>, PI(4,5)P<sub>2</sub>, PI(3,4,5)P<sub>3</sub>, and PIPN(control));  $n = 3$ . (D) The PH domain of  $\beta$ II-spectrin is sufficient to target to the plasma membrane. 25 ng of plasmids was transfected into MDCK cells grown on 14-mm MatTek plates. Top, the XZ plane; bottom, the XY plane. (E)  $\beta$ II-Spectrin knockdown cells were transfected with K2207Q GFP- $\beta$ II-spectrin (green,  $\alpha$ -GFP; red,  $\alpha$ -ankyrin-G; white,  $\alpha$ -ZO-1). (F) Quantification of lateral membrane heights rescued by WT or K2207Q GFP- $\beta$ II-spectrin. Results were analyzed using Student's  $t$  test; \*,  $P < 0.001$ ;  $n = 19$ –21. (G) 1  $\mu\text{g}$  of plasmids encoding PH domain from PLC $\delta$ 1 (GFP-PLC $\delta$ 1-PHD) or  $\beta$ II-spectrin (GFP- $\beta$ II-spectrin-PHD) was transfected in MDCK cells grown on 14-mm MatTek plates (green,  $\alpha$ -GFP; red,  $\alpha$ - $\beta$ II-spectrin). Bars, 10  $\mu\text{m}$ . (H) Quantification of the height of lateral membranes and the disassociation of endogenous  $\beta$ II-spectrin from plasma membrane under each experimental condition. Results were analyzed using one-way ANOVA and Tukey's tests; \*,  $P < 0.001$ ; mean  $\pm$  SEM;  $n = 31$ –36.

The finding that DAR999AAA ankyrin-G mutant remains on the lateral membrane (Fig. 6, B and D) suggests that ankyrin-G does not require  $\beta$ II-spectrin for targeting to the lateral membrane. To further test this conclusion, we evaluated the localization of endogenous ankyrin-G in the absence of  $\beta$ II-spectrin (Fig. 7 A). Consistently, in  $\beta$ II-spectrin knockdown cells, ankyrin-G remains on the lateral membrane (Fig. 7, E and F, WT). Mutation of a highly conserved tyrosine located in a surface-exposed loop within the 15th repeat of  $\beta$ -spectrins disrupts their interaction with ankyrins (Kizhatil et al., 2007b; Ipsaro et al., 2009; Ipsaro and Mondragón, 2010; Fig. 7, B and C).

We confirmed that the Y1874A mutation increased the dissociation constant of  $\beta$ II-spectrin for ankyrin-G from 10–20 nM to >200 nM, and thus reduced the affinity by at least eightfold (Fig. 7 D). In addition, we also confirmed that this mutant still retained the same lipid-binding activity as WT  $\beta$ II-spectrin (Fig. S2 D). GFP-tagged Y1874A  $\beta$ II-spectrin was mislocalized to the apical membrane and also failed to restore the lateral membrane height compared with the WT (Fig. 7, E and F, Y1874A). This is consistent with our finding that endogenous  $\beta$ II-spectrin requires ankyrin-G to maintain its polarized targeting to the lateral membrane (Fig. 6, B and D).

**Figure 9. DHHC5/8 and  $\beta$ II-spectrin colocalize with ankyrin-G in microdomains.** The immunostaining of DHHC5/8,  $\beta$ II-spectrin, or ankyrin-G on the lateral membrane was analyzed using 3D deconvolution method in Velocity Image Analysis Software. Shown here are the en face views of the lateral membrane. Bars, 5  $\mu$ m. (A) GFP-tagged DHHC5 or 8 were transfected into MDCK cells (green,  $\alpha$ -GFP; red,  $\alpha$ -ankyrin-G). (B) WT or Y1874A GFP- $\beta$ II-spectrin was expressed in  $\beta$ II-spectrin-silenced MDCK cells (green,  $\alpha$ -GFP; red,  $\alpha$ -ankyrin-G). (C) WT or DAR999AAA ankyrin-G-GFP was expressed in ankyrin-G-silenced MDCK cells (green,  $\alpha$ -GFP; red,  $\alpha$ - $\beta$ II-spectrin). (D) DAR999AAA ankyrin-G-GFP and HA-DHHC5 were coexpressed in ankyrin-G-silenced MDCK cells (green,  $\alpha$ -GFP; red,  $\alpha$ -HA). (E) Quantification of the colocalization indicated by Pearson coefficients. Student *t* test; \*, *P* < 0.01; mean  $\pm$  SEM; *n* = 4–7.



We then performed FRAP experiments to examine whether loss of ankyrin-G- $\beta$ II-spectrin interaction affects their higher-order assembly into stabilized structures. Indeed, the Y1874A GFP- $\beta$ II-spectrin exhibited a marked increase in dynamics on the lateral membrane compared with the WT GFP- $\beta$ II-spectrin (Fig. 7 G), affecting both the extent of recovery (55% for WT and 86% for Y1874A) and half-life (36 s for WT and 17 s for Y1874A). Even though ankyrin-G does not require binding to  $\beta$ II-spectrin to maintain its polarized localization based on our immunofluorescence study, it does require  $\beta$ II-spectrin binding for its proper dynamics (Fig. 7 G; recovery percentage: WT 38% and DAR999AAA 80%; half-life: WT 40 s and DAR999AAA 32 s). These results indicate that ankyrin-G and  $\beta$ II-spectrin depend on each other for their dynamics and function in MDCK cells.

The nonpolarized plasma membrane association of Y1874A  $\beta$ II-spectrin is likely caused by its PH domain because the  $\beta$ II-spectrin PH domain fused to GFP also associates generically with all plasma membrane surfaces (Fig. 8 D). We next addressed the role of phosphoinositide recognition by the PH domain of  $\beta$ II-spectrin. Basic residues in the PH domain of

$\beta$ -spectrin required for binding to inositol (1,4,5) $P_3$  have been identified using nuclear magnetic resonance and other methods (Hyvönen et al., 1995; Rameh et al., 1997). Moreover, mutation of a basic PH domain residue eliminated binding of *Drosophila*  $\beta$ -spectrin to PI(4,5) $P_2$  (Das et al., 2008). We confirmed that K2207Q mutation in the PH domain of  $\beta$ II-spectrin abolished binding affinity for phosphoinositides based on loss of interaction with lipid strips and liposomes containing various phosphoinositide lipids (Fig. 8 C and Fig. S2 C). WT  $\beta$ II-spectrin also associated with PI(3,4) $P_2$  and PI(3,4,5) $P_3$  in addition to PI(4,5) $P_2$ , and these interactions were also eliminated by the K2207Q mutation.

The K2207Q  $\beta$ II-spectrin mutant exhibited a striking loss of association with the plasma membrane and remained intracellular (Fig. 8 E), whereas endogenous ankyrin-G under these conditions remains on the residual lateral membrane. The K2207Q  $\beta$ II-spectrin mutant also failed to restore the lateral membrane height (Fig. 8, E and F). This loss of plasma membrane targeting of K2207Q  $\beta$ II-spectrin, which still retains ankyrin-G binding activity (Fig. S2, A and B), is not consistent with a simple linear assembly pathway. Instead,  $\beta$ II-spectrin association

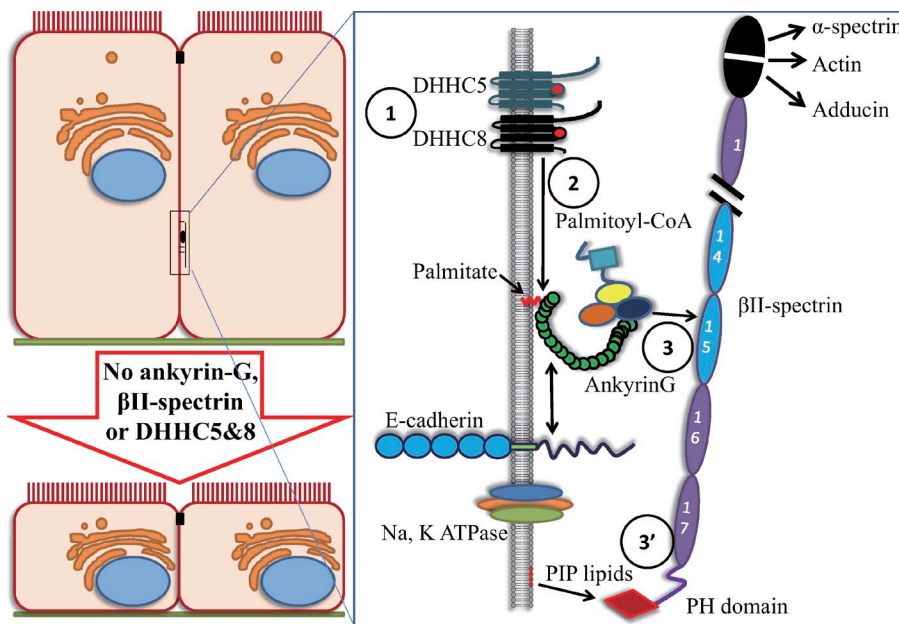


Figure 10. **A DHHC5/8-ankyrin-G- $\beta$ II-spectrin network is required to build lateral membranes of polarized MDCK cells.** The schematic view summarizes roles of DHHC5/8, ankyrin-G, and  $\beta$ II-spectrin in assembling the lateral membrane of columnar epithelial cells. DHHC5/8 are localized to the lateral membrane, where they palmitoylate ankyrin-G.  $\beta$ II-Spectrin requires coincidence detection of ankyrin-G and phosphoinositide lipids to ensure its precise lateral membrane localization. Loss of any of the components or the functional relationship results in reduced lateral membrane height.

with ankyrin-G on the lateral membrane is somehow coupled to interactions of its PH domain with phosphoinositide lipids. The dual requirement of  $\beta$ II-spectrin for both ankyrin and phosphoinositide lipids may explain some of the complexity noted in earlier analysis of relationships between ankyrins and spectrin in *Drosophila* (Das et al., 2008).

In our lipid binding assays, even though  $\beta$ II-spectrin showed the highest binding activity with  $PI(4,5)P_2$  lipids, it also bound to  $PI(3,4)P_2$  and  $PI(3,4,5)P_3$  and the binding to these lipids is abolished by the K2207Q mutation (Fig. 8 C). Because  $PI(4,5)P_2$  is enriched in the apical domain, whereas  $PI(3,4,5)P_3$  confers basolateral membrane identity in some epithelial cell models (Gassama-Diagne et al., 2006; Martin-Belmonte et al., 2007; Shewan et al., 2011), we next decided to examine whether  $\beta$ II-spectrin acts through  $PI(4,5)P_2$ . Overexpression of the PH domain from phospholipase C  $\delta 1$ , which specifically binds to  $PI(4,5)P_2$  but not  $PI(3,4)P_2$  or  $PI(3,4,5)P_3$  (Razzini et al., 2000), showed strong apical localization but was not excluded from lateral membranes (Fig. 8 G). Overexpression of this  $PI(4,5)P_2$ -specific PH domain showed no significant defects in either the lateral localization of  $\beta$ II-spectrin or the cell height (Fig. 8, G and H). However, overexpression of the PH domain from  $\beta$ II-spectrin showed no enrichment on the apical membrane (Fig. 8 G). More interestingly, overexpression of the  $\beta$ II-spectrin PH domain disrupted the plasma membrane localization of  $\beta$ II-spectrin and also significantly reduced the membrane height (Fig. 8, G and H). Together these findings suggest that  $\beta$ II-spectrin requires  $PI(3,4)P_2$  and  $PI(3,4,5)P_3$  but not  $PI(4,5)P_2$  for its lateral membrane localization and function.

#### DHHC5/8, ankyrin-G, and $\beta$ II-spectrin colocalize in micrometer-scale membrane subdomains

We next examined the spatial relationships among DHHC5/8, ankyrin-G, and  $\beta$ II-spectrin in the lateral membrane using 3D deconvolution to improve resolution of confocal microscopy

(Sibarita, 2005; Santangelo et al., 2009; Biggs, 2010). To evaluate DHHC5/8 and native ankyrin-G at steady-state, MDCK cells were transfected with GFP-DHHC5 or 8, fixed, and costained with antibodies against GFP and ankyrin-G. After 3D restoration and deconvolution of a selected lateral membrane region (Fig. S3 A), we observed subdomains containing DHHC5/8 or ankyrin-G that ranged in size from  $0.5\text{--}2\ \mu\text{m}^2$  (Fig. 9 A). We further confirmed this micropattern by examining live cells expressing GFP-tagged ankyrin-G or  $\beta$ II-spectrin (Fig. S3, B and C). In contrast, subdomains were not observed in live cells incubated with small lipophilic probes, which uniformly labeled the lateral membrane (Fig. S3 D).

Substantial populations of DHHC5 and -8 are copatterned with ankyrin-G-positive microdomains based on Pearson coefficients of 0.7 for DHHC5/ankyrin-G and 0.6 for DHHC8/ankyrin-G (Fig. 9, A and E). WT  $\beta$ II-spectrin also copatterned with ankyrin-G-positive microdomains (Fig. 9 B, WT). To further evaluate the colocalization between ankyrin-G and  $\beta$ II-spectrin, we replaced endogenous  $\beta$ II-spectrin with either WT or Y1874A mutant GFP- $\beta$ II-spectrin. This colocalization of  $\beta$ II-spectrin with ankyrin-G required ankyrin-spectrin interaction because the Y1874A  $\beta$ II-spectrin mutant-ankyrin-G exhibited a markedly reduced Pearson coefficient of 0.3 compared with 0.8 for WT ankyrin-G- $\beta$ II-spectrin (Fig. 9, B and E). However, Y1874A  $\beta$ II-spectrin mutant is still patterned into microdomains, probably through its PH domain or other unidentified protein interactions. Similarly, we replaced endogenous ankyrin-G with either WT or DAR999AAA ankyrin-G-GFP and evaluated their colocalization with endogenous  $\beta$ II-spectrin. DAR999AAA ankyrin-G and  $\beta$ II-spectrin showed significantly reduced colocalization with a Pearson coefficient of 0.3 compared with 0.8 for WT ankyrin-G (Fig. 9, C and E). We hypothesized that the colocalization of ankyrin-G and DHHC5 or -8 in those microdomains is mediated by palmitoylation. Because the C70A ankyrin-G showed minimal membrane localization in ankyrin-G knockdown cells (Fig. 7 B),

it was not possible to examine the micropatterning of C70A ankyrin-G. However, when we examined the DAR999AAA ankyrin-G, which is still palmitoylated (unpublished data), it showed markedly reduced colocalization with DHHC5 (Fig. 9, D and E). This finding was surprising but consistent with the fact that cells require all the components and functional connection among DHHC5/8, ankyrin-G, and  $\beta$ II-spectrin to build the lateral membrane. Thus MDCK cells require both palmitoylation and protein interactions to properly assemble their microdomains.

The finding that DHHC5/8 and  $\beta$ II-spectrin are copatterned with ankyrin-G into highly organized microdomains suggests a model where ankyrin-G is locally palmitoylated at the lateral membrane, and in turn drives the polarized recruitment of  $\beta$ II-spectrin–phosphoinositide complexes (Fig. 9). Loss of ankyrin-G– $\beta$ II-spectrin interaction as a result of mutation of either protein results in loss of ankyrin-G– $\beta$ II-spectrin copatterning in those microdomains and failure to restore the epithelial lateral membrane. Thus recruitment of  $\beta$ II-spectrin to ankyrin-G microdomains is essential for its downstream functions in building lateral membranes.

## Discussion

This study identifies two critical inputs from lipids that together provide a rationale for how ankyrin-G and  $\beta$ II-spectrin selectively localize on lateral membranes of MDCK epithelial cells (Fig. 10). These experiments began with the observation that ankyrin-G is S-palmitoylated at a single conserved cysteine that is required for ankyrin-G function in assembling lateral membranes and axon initial segments (He et al., 2012). Here, we identified DHHC palmitoyltransferases 5 and 8 as the DHHC family members required for ankyrin-G palmitoylation as well as its localization at the lateral membranes of polarized MDCK cells. We also found that  $\beta$ II-spectrin functions as a coincidence detector that requires recognition of both palmitoylated ankyrin-G and phosphoinositide lipids as a prerequisite for its localization to the lateral membrane (Figs. 8 and 9). DHHC5/8 and phosphoinositides thus ensure that ankyrin-G and  $\beta$ II-spectrin localize only on lateral plasma membranes and not in the cytosol or on other membrane surfaces. Loss of either DHHC5 or -8, interactions between ankyrin-G and  $\beta$ II-spectrin, or  $\beta$ II-spectrin recognition of phosphoinositide lipids all result in failure to build the lateral membrane, which underscores the functional importance of this pathway.

Our findings establish DHHC5 and -8 as critical determinants of polarity for ankyrin-G and  $\beta$ II-spectrin in MDCK cells. However, the mechanisms responsible for polarized localization of DHHC5 and -8 themselves at the lateral membrane remain to be elucidated. Both proteins are distinguished from other DHHC family members by an extended cytoplasmic domain (Thomas et al., 2012). However, substitution of the C-terminal domain of DHHC14 for that of DHHC5 does not abolish lateral membrane targeting of DHHC5 (Fig. S4). Thus, important localization information resides in the N-terminal halves of DHHC5 and -8.

The finding that  $\beta$ II-spectrin requires both ankyrin-G and phosphoinositides to associate with the lateral membrane was unexpected given the high affinity of the ankyrin-G– $\beta$ II-spectrin

interaction (Fig. 7 D). In contrast to erythrocytes, where  $\beta$ -spectrin lacks a PH domain because of alternative splicing but is tightly bound to the plasma membrane through ankyrin (Bennett and Stenbuck, 1979; Byers and Branton, 1985; Winkelmann et al., 1990), in MDCK cells the ankyrin–spectrin protein interaction is somehow coordinated with protein–lipid interactions. An advantage of imposing a dual requirement for phosphoinositides in addition to ankyrin binding is to prevent association of  $\beta$ -spectrins with ankyrin at sites other than the plasma membrane.

A critical tool that we developed for this study was a method to generate inducible shRNA-mediated knockdown of protein expression in an entire population of MDCK cells. This permitted evaluation of the roles of ankyrin-G and  $\beta$ II-spectrin in assembling lateral membranes without interference caused by other cellular defects, including impaired cytokinesis caused by loss of ankyrin-G or  $\beta$ II-spectrin (Hu et al., 1995). Previous research using a transient siRNA strategy that resulted in a nearly complete loss of ankyrin-G in human bronchial epithelial cells also led to a complete loss of the lateral membrane domain accompanied by intracellular accumulation of E-cadherin (Kizhatil and Bennett, 2004; Kizhatil et al., 2007a,b). However, we did not observe either complete loss of the lateral membrane or intracellular accumulation of E-cadherin in MDCK cells with 80–90% knockdown achieved with the inducible system. We conclude that the intracellular accumulation of E-cadherin likely was secondary to elimination of sites for exocytosis because of complete loss of lateral membranes rather than a failure of post-Golgi transport as originally proposed (Kizhatil et al., 2007a).

Although DHHC5/8, ankyrin-G, and  $\beta$ II-spectrin are required for columnar morphology of MDCK cells and operate in the same pathway, the mechanism of action of these proteins in expanding the lateral membrane remains to be determined. One possibility is that a lateral membrane–associated spectrin-based actin skeleton provides mechanical support for epithelial monolayers by coupling to membrane-spanning cell adhesion molecules such as E-cadherin, which is an ankyrin-G partner (Nelson et al., 1990a,b; Kizhatil et al., 2007b). Another possibility is that an ankyrin-G–spectrin–actin skeleton promotes cell height by enhancing cell–cell contacts through retention of E-cadherin and prevention of its endocytosis. In support of this idea, E-cadherin polarity in MDCK cells depends on a motif in its cytoplasmic domain that contains both ankyrin-binding activity as well as embedded dileucine residues required to engage clathrin endocytosis (Jenkins et al., 2013). E-cadherin likely can associate with either ankyrin-G or clathrin adaptors but not both at the same time, and thus is restricted to the lateral membrane by the ankyrin–spectrin skeleton. A surprising conclusion of our study is that E-cadherin interaction with ankyrin-G is not sufficient to recruit ankyrin-G to the lateral membrane, which also requires palmitoylation in addition to its protein interactions. However, once ankyrin-G concentrates at the lateral membrane it may be able to prevent participation of E-cadherin in endocytosis through competition for binding to the polarity motif. Interestingly, inhibition of endocytosis of the cell adhesion molecule Fas2 has been proposed as a mechanism for regulating cell height in *Drosophila* epithelia (Gomez et al., 2012).

We have observed for the first time that ankyrin-G and  $\beta$ II-spectrin are concentrated in microdomains ranging from 0.5 to 2  $\mu\text{m}^2$  in the MDCK cell lateral membrane (Fig. 9), which is inconsistent with the conventional view of a uniform ankyrin-spectrin lattice as observed in the plasma membrane of erythrocytes (Liu et al., 1987; Bennett and Baines, 2001; Baines, 2010). We believe that microdomains are not an artifact of cell fixation or deconvolution software because we observe similar micro-patterning using live imaging with ankyrin-G-GFP and GFP- $\beta$ II-spectrin as with fixed cells (Fig. S3, B and C). In contrast, imaging with a lipid probe reveals uniform labeling (Fig. S3 D). Moreover, the protein interaction-dependent colocalization between ankyrin-G and  $\beta$ II-spectrin demonstrates specificity in cosegregation of these proteins (Fig. 9, B and C). The ankyrin-G and  $\beta$ II-spectrin microdomains revealed by 3D deconvolution microscopy in our study are distinguishable from membrane lipid rafts, which normally are much smaller (Lingwood and Simons, 2010; Simons and Gerl, 2010). Segregation of functionally related proteins into microdomains can provide a platform for proteins that interact with moderate affinity and require high local concentration to achieve complexes. The fact that DHH5 and -8 colocalize with ankyrin-G in these microdomains suggests these microdomains are sites of palmitoylation of ankyrin-G.

In summary, we have identified functional interactions connecting palmitoyltransferases DHH5 and -8 with their substrate ankyrin-G, ankyrin-G with its partner  $\beta$ II-spectrin, and  $\beta$ II-spectrin with phosphoinositide lipids that are all required to build lateral membranes of MDCK columnar epithelial cells. Given the rapidly reversible nature of palmitoylation (Rocks et al., 2010; Martin et al., 2012; Fukata et al., 2013), as well as phosphoinositides synthesis and degradation (Di Paolo and De Camilli, 2006; Shewan et al., 2011), these new findings suggest that the ankyrin-G- $\beta$ II-spectrin-based membrane skeleton is much more dynamic and subject to regulation than previously appreciated. Moreover, the regulatory network properties of this set of interactions in terms of positive and negative feedback and coincidence circuitry are important areas for future investigation. Finally, our findings reinforce an emerging view of plasma membrane identity determination by a combinatorial code based on highly dynamic protein and lipid variables rather than hard-wired stable protein assemblies.

## Materials and methods

### Plasmids

The 23 HA-tagged mouse DHH constructs (the DHH cDNA sequences were cloned into pEF-BOS-HA backbone using BamHI cut sites and under control of pEF-1  $\alpha$  promoter) were a gift from M. Fukata (National Institute for Physiological Sciences, Okazaki, Japan). DHH5 was subcloned into peGFP-C1 vector using SacII and BamHI cut sites; DHH8 was subcloned into peGFP-C1 vector using Sall and BamHI cut sites; DHH14 was subcloned into peGFP-N1 using HindIII and EcoRI cut sites. The WT ankyrin-G-GFP and mutants C70A and DAR999AAA were previously described (Kizhatil et al., 2007b; He et al., 2012, 2013) and the sequences were cloned into peGFP-N1 using EcoRI and Sall cut sites. The human  $\beta$ II-spectrin cDNA was subcloned into peGFP-C3 vector using HindIII and SacII cut sites and the mutations Y1874A and K2207Q were introduced by mutagenesis. For  $\beta$ II-spectrin purification, a prescission protease site (LEVLFGQP) was introduced between the GFP and start codon. The PH domain of

human  $\beta$ II-spectrin (amino acids 2200–2305) was subcloned into peGFP-N1 using XhoI and SacII cut sites.

### Reagents and antibodies

Palmitic acid, [9,10- $^3\text{H}$ (N)] (PerkinElmer); N-ethylmaleimide and hydroxylamine (Sigma-Aldrich); EZ-Link BMCC-Biotin (Thermo Fisher Scientific); Dynabeads with protein G and Lipofectamine 2000 transfection reagent (Invitrogen); and the QuikChange II XL Site-Directed Mutagenesis kit (Agilent Technologies) were used. Mouse  $\alpha$ -HA monoclonal antibody (Santa Cruz Biotechnology, Inc.); rabbit  $\alpha$ -GFP polyclonal antibody (laboratory generated); chicken  $\alpha$ -GFP polyclonal antibody, rat  $\alpha$ -E-cadherin monoclonal antibody (Abcam); rabbit or goat  $\alpha$ -ankyrin-G polyclonal antibody (laboratory generated using the C-terminal domain as epitope); rabbit  $\alpha$ - $\beta$ II-spectrin polyclonal antibody (laboratory generated using repeat 4–9 as epitope); rabbit  $\alpha$ -biotin polyclonal antibody, rabbit  $\alpha$ -DHH5 polyclonal antibody, and rabbit  $\alpha$ -DHH8 polyclonal antibody (Abcam); mouse  $\alpha$ -GAPDH monoclonal antibody (Sigma-Aldrich); and mouse  $\alpha$ -ZO-1 monoclonal antibody (Invitrogen) were used.

### Metabolic radiolabeling

This assay was performed following the protocol previously described with a few modifications (Fukata et al., 2006). In brief,  $10^6$  HEK293T cells were plated in the 6-well plates and transfected with 2  $\mu\text{g}$  HA-DHH plasmids plus 3  $\mu\text{g}$  ankyrin-G-GFP plasmids. 20 h after transfection, the cells were incubated with DMEM supplemented with 5% dialyzed FBS for 1 h, then [ $^3\text{H}$ ]palmitic acid was added to the final concentration of 200  $\mu\text{Ci}/\text{ml}$ . After 4-h incubation, the cells were washed with PBS and lysed directly using 0.5 ml SDS-PAGE buffer (62.5 mM Tris-HCl, pH 6.8, 10% glycerol, 2% SDS, 0.001% bromophenol blue, and 10 mM DTT) and heated for 5 min at 70°C. The proteins were separated in 3.5–17.5% gradient polyacrylamide gels. For Western blotting, samples were transferred onto nitrocellulose membrane and probed with  $\alpha$ -GFP or  $\alpha$ -HA antibody. For autoradiography, the gels were treated with amplify fluorographic reagent, dried using cellophane membrane, and exposed to x-ray film at  $-80^\circ\text{C}$ .

### Generation of doxycycline-inducible shRNA MDCK cell lines

The original pLKO-Tet-on lentiviral vector (Addgene) was modified by replacement of the puromycin resistant gene with fluorescent TagBFP and the internal ribosome entry site with P2A peptide (5'-GSGATNFSLLKQAGDVEENPGP-3'), which mediates cotranslational cleavage. After cloning the shRNA hairpin targeting genes of interest to the vector, lentivirus was generated following standard protocol (Wiederschain et al., 2009). On the day of infection,  $0.5$ – $10^6$  MDCK cells were mixed with virus and 8  $\mu\text{g}/\text{ml}$  polybrene and plated in 6-well dishes. 16 h later, the cells were extensively washed to remove viral particles and then grown in DMEM and 10% FBS. The next day, cells were trypsinized and sorted for the brightest TagBFP population ( $\sim 1\%$ ), which can be maintained as a stable cell line. Hairpins used to target genes of interest were as follows: luciferase control (5'-GGAGATCGAATCTTAATGTGC-3'), dog ankyrin-G (5'-GCTAGAAGTAGCTAATCTCCT-3'), dog  $\beta$ II-spectrin (5'-GGTGCTATTATCTCAAGA-3'), dog DHH5 (5'-GTGTCAGATGGGCAGATAACT-3'), dog DHH8 (5'-ACCTGTCCAGGACCATCATGG-3'), and dog DHH5/8 (5'-TGGGTGAACAACCTGTATCG-3').

### RT-PCR

To examine the native transcription of DHH5 and DHH8 in MDCK cells, total RNA was isolated using standard TRIzol-based protocol, and cDNA was generated using SuperScript III First-Strand Synthesis System (Life Technologies). Primers used for gene amplification were dog GAPDH (forward: 5'-GGTGATGCTGGTGCTGAGTATGTTG-3'; reverse: 5'-AGTGAAGCAGGGATGATGTTCTGG-3'), dog DHH5 (forward: 5'-GGAGGATGAAGACAAGGAAGATGAC-3'; reverse: 5'-GCTACAGGATGAAGAATAAGCCAG-3'), and dog DHH8 (forward: 5'-GATGAGGACGAGGATAAGGAGGAC-3'; reverse: 5'-GATGACAGGGATGAAGAGGC-3').

### Acyl-biotin exchange assay

This assay was previously described (He et al., 2012). In brief, Luc-, DHH5-, DHH8-, or DHH5/8-shRNA cells were induced by 4  $\mu\text{g}/\text{ml}$  doxycycline for 3 d and then homogenized in the presence of 50 mM N-ethylmaleimide. 1% SDS was added to the lysates to increase ankyrin-G solubility. After sonication and centrifugation, Triton X-100 was added to a final concentration of 1% (vol/vol) to quench SDS. 60  $\mu\text{l}$  of dynabeads preloaded with 10  $\mu\text{g}$   $\alpha$ -ankyrin-G antibody were then incubated with the lysates overnight. The beads were then washed and incubated with hydrolysis-labeling buffer (1 M hydroxylamine/Tris as a control, 80  $\mu\text{M}$  BMCC-biotin, 10 mM sodium phosphate, and 2 mM Na-EDTA, pH 7) at room temperature

for 2 h. Beads were then washed and incubated with loading buffer (2% SDS, 10% glycerol, 40 mM Tris-HCl, 150 mM NaCl, 2 mM NaEDTA, and 200 mM DTT with Bromophenol blue). Samples were analyzed by SDS-PAGE and probed by immunoblotting with  $\alpha$ -ankyrin-G or  $\alpha$ -biotin antibodies. The total cell lysates were also collected and analyzed to confirm the knockdown efficiency of DHHc5 and -8.

### Transfection and Immunofluorescence

To examine the subcellular localization of the 23 DHHc palmitoyltransferases,  $10^5$  MDCK cells were plated in the insert of MatTek plates. The next day, cells were transfected with 80 ng of plasmids encoding HA- or GFP-DHHc using Lipofectamine. 48 h later, the cells were fixed by 4% PFA for 15 min, permeabilized by 0.4% Triton X-100 for 10 min, blocked by 5% BSA, and incubated with primary antibody overnight at 4°C. Alexa Fluor 488 and 568 were used for secondary antibody. To study the localization of ankyrin-G after silencing DHHc5, DHHc8, or DHHc5/8, cells were induced by 4  $\mu$ g/ml doxycycline for one day and then replated on MatTek plates in the presence of doxycycline for another 2 d before fixation. Parallel samples were collected for Western blotting to study ankyrin-G levels. To stain endogenous  $\beta$ -spectrin in MDCK cell, we used 1% PFA at 4°C for 1 h and then followed the protocol as described above.

### Calcium switch assay and lateral membrane reassembly

The calcium switch assay was previously described (He et al., 2012). Here we used this assay to study lateral membrane reassembly. Luc-, Ankyrin-G-, or DHHc5/8-shRNA cells were induced by 4  $\mu$ g/ml doxycycline for 3 d, and then trypsinized and plated in calcium-depleted medium (DMEM, 5% dialyzed FBS, and 4  $\mu$ g/ml doxycycline;  $10^6$  cells in MatTek plates). The next day, the plates were washed slightly to remove unattached cells and then switched to regular medium (DMEM, 10% FBS, and 4  $\mu$ g/ml doxycycline). Cells were then fixed at different time points (2, 4, 8, 16, and 24 h). To examine the localization of transfected GFP-DHHc5 and -8 in unpolarized MDCK cells, 100 ng DNA was transfected into MDCK cells following standard protocol. 6 h later, the cells were trypsinized and replated in calcium-depleted medium and kept for 24 h before fixation.

### Lateral membrane rescue

$10^7$  ankyrin-G-shRNA or  $\beta$ -spectrin-shRNA cells were induced in 10-cm dishes in the presence of 4  $\mu$ g/ml doxycycline for 16 h. Then  $1.5 \times 10^5$  pre-induced cells were replated in MatTek plates. 8 h later, cells were washed and transfected with 100 ng of rescue plasmids (GFP, Ankyrin-G-GFP, or GFP- $\beta$ -spectrin) using the standard protocol. Cells were maintained in 4  $\mu$ g/ml doxycycline and fixed 48 h after transfection.

### Microscopy

Imaging for fixed samples was performed at room temperature using an inverted confocal microscope (LSM780; Carl Zeiss) with camera (AxioCam MRm Rev.3) and 63 $\times$ , NA 1.40, or 100 $\times$ , NA 1.45 oil objective lenses. Secondary antibodies were conjugated with Alexa Fluor 488, 568, or 647. XZ planes were reconstructed from Z stacks with optical sections of 250 nm using ZEN 2012 software. For live imaging, the incubation chamber was maintained at 37°C, 5% CO<sub>2</sub>, and cells were maintained in growth medium (DMEM and 10% FBS). For 3D deconvolution microscopy, images were collected at room temperature using the 100 $\times$ , NA 1.45, objective lens with optical sections of 250 nm and subjected to 3D deconvolution in Volocity 3D Image Analysis Software (PerkinElmer) with a point spread function (axial spacing in Z: 0.25  $\mu$ m; lateral spacing in XY: 0.0277  $\mu$ m; medium reference index: 1.52; NA 1.45; detector pinhole size: 1 Airy unit).

### Expression and purification of $\beta$ -spectrin

$\beta$ -spectrin was cloned into pEGFP-C3 along with a precision protease site (LEVLFGGP) between the GFP and ATG of  $\beta$ -spectrin. Mutations were made into the  $\beta$ -spectrin sequence using site-directed mutagenesis (Agilent Technologies). WT  $\beta$ -spectrin and mutants were transfected into 293T17 cells in 10-cm dishes using lipofectamine (Invitrogen). After 36 h, lysates were produced from each transfection and GFP- $\beta$ -spectrin was isolated using a rabbit anti-GFP antibody and pulled down using protein G dynabeads (Invitrogen). After extensive washing using high salt and Triton X-100,  $\beta$ -spectrin was released from dynabeads using precision protease enzyme (GE Healthcare).

### Ankyrin-G- $\beta$ -spectrin binding assay

His-tagged ankyrin-G expressed in S9 cells was purified as previously described (Kizhatil et al., 2007a). In brief, S9 cells expressing ankyrin-G-His using the pBacPak9 system were lysed in 50 mM phosphate buffer, 0.3 M

NaBr, 20 mM imidazole, and 0.2 mM  $\beta$ -mercaptoethanol and coupled to nickel Sepharose (GE Healthcare). Sepharose was washed with binding buffer, and proteins were finally eluted in buffer containing 50 mM phosphate buffer, 0.3 M NaBr, and 70 mM imidazole. WT GFP- $\beta$ -spectrin and Y1874A GFP- $\beta$ -spectrin expressed and purified from HEK293 cells were immobilized using an antibody against GFP on protein G dynabeads and increasing concentrations of ankyrin-G-His were added to a final reaction volume of 200  $\mu$ l in binding buffer (10 mM sodium phosphate, 75 mM NaCl, 1 mM DTT, 1 mM EDTA, 5% sucrose, and 4% BSA, pH 7.3). Bound and free ankyrin-G-His were separated by pelleting beads through a 20% sucrose cushion. The amount of bound ankyrin-G-His was determined through immunoblotting with  $\alpha$ -His antibody followed by phosphorimager analysis. Data points were generated after normalization for  $\beta$ -spectrin levels and nonspecific binding of ankyrin-G.

### FRAP

300 ng of plasmids encoding WT or Y1874A GFP- $\beta$ -spectrin were transfected into  $\beta$ -spectrin-silenced MDCK cells as described in Lateral membrane rescue. Similarly, WT or DAR999AAA ankyrin-G-GFP were transfected into ankyrin-G-silenced cells. The GFP signals were collected every 5 s for a 3-min period. At each time point, three regions were monitored: region 1 is the photobleached membrane area; region 2 is a membrane area of an adjacent transfected cell, which can be used to control the signal variability; region 3 is a nontransfected cell region, which is used to correct the background noise. The signal from region 1 was double normalized to that from regions 2 and 3, and then fitted to the exponential equation  $y = y_0 + Ae^{-kx}$ .

### Phosphatidylinositol binding assay

We purchased phosphatidylinositol-labeled liposomes that contained a biotin tag from Echelon Biosciences. Liposomes for PIP<sub>2</sub>(3,4), PIP<sub>2</sub>(4,5), PIP<sub>3</sub>(3,4,5), and PIPN(control) were used at 10- $\mu$ M concentration and incubated with purified WT  $\beta$ -spectrin and K2207Q  $\beta$ -spectrin in interaction buffer (50 mM Tris, 100 mM NaCl, 1 mM DTT, 5% sucrose, and 3% fatty acid-free BSA, pH 7.4). Bound  $\beta$ -spectrin was separated from free  $\beta$ -spectrin through pull-down of liposomes using streptavidin-labeled dynabeads. Levels of protein binding were determined by immunoblotting using  $\alpha$ - $\beta$ -spectrin antibody and quantified through phosphorimager.

### Data analysis

ImageJ was used to measure the fluorescence intensity of confocal microscopy images. To measure the mean intensity of the plasma membrane, a line was drawn along the plasma membrane and recorded. To measure the mean intensity of cytoplasm, an area of interest was drawn within the cytoplasm and recorded. A Typhoon 9200 phosphorimager and Imagequant software (GE Healthcare) were used to quantify the intensity of Western blots. Student's *t* test was used to analyze two-group comparisons, and one-way analysis of variance (ANOVA) followed by Tukey's tests were used to perform multiple group comparisons. The tests were performed using Prism 5 software (GraphPad Software).

### Online supplemental material

Fig. S1 A shows that C70A ankyrin-G is resistant to palmitoylation. Fig. S1 B shows that silencing DHHc5 does not up-regulate the level of DHHc8 and vice versa. Fig. S1 (C and D) shows that the protein level of DHHc5 or 8 is not altered during the polarization process of MDCK cells. Fig. S1 E shows that loss of DHHc5/8 results in plasma membrane dissociation of ankyrin-G in unpolarized MDCK cells. Fig. S2 (A and B) shows that C70A ankyrin-G and K2207Q  $\beta$ -spectrin maintain their protein binding activities. Fig. S2 (C and D) shows that Y1874A  $\beta$ -spectrin maintains its lipid binding activity. Fig. S2 E shows that  $\beta$ -spectrin is mislocalized in DHHc5/8 silenced MDCK cells. Fig. S3 shows that the micropatterning of ankyrin-G or  $\beta$ -spectrin exists in live cells. Fig. S4 shows that the C terminus of DHHc5 is not required for its lateral localization. Online supplemental material is available at <http://www.jcb.org/cgi/content/full/jcb.201401016/DC1>. Additional data are available in the JCB DataViewer at <http://dx.doi.org/10.1083/jcb.201401016.dv>.

We gratefully acknowledge Dr. Masaki Fukata for offering all 23 constructs of DHHc palmitoyltransferases. We also thank Dr. Michael Cook from the Duke cell-sorting facility for his assistance in cell sorting and Dr. Paul Jenkins for his efforts in setting up the 3D deconvolution microscopy.

The authors declare no competing financial interests.

Submitted: 6 January 2014

Accepted: 17 June 2014

## References

- Baines, A.J. 2010. The spectrin-ankyrin-4.1-adducin membrane skeleton: adapting eukaryotic cells to the demands of animal life. *Protoplasma*. 244:99–131. <http://dx.doi.org/10.1007/s00709-010-0181-1>
- Bartels, D.J., D.A. Mitchell, X. Dong, and R.J. Deschenes. 1999. Erf2, a novel gene product that affects the localization and palmitoylation of Ras2 in *Saccharomyces cerevisiae*. *Mol. Cell Biol.* 19:6775–6787.
- Bennett, V., and P.J. Stenbuck. 1979. Identification and partial purification of ankyrin, the high affinity membrane attachment site for human erythrocyte spectrin. *J. Biol. Chem.* 254:2533–2541.
- Bennett, V., and A.J. Baines. 2001. Spectrin and ankyrin-based pathways: metazoan inventions for integrating cells into tissues. *Physiol. Rev.* 81: 1353–1392.
- Bennett, V., and J. Healy. 2009. Membrane domains based on ankyrin and spectrin associated with cell–cell interactions. *Cold Spring Harb. Perspect. Biol.* 1:a003012. <http://dx.doi.org/10.1101/cshperspect.a003012>
- Bennett, V., and D.N. Lorenzo. 2013. Spectrin- and ankyrin-based membrane domains and the evolution of vertebrates. *Current Top. Membr.* 72:1–37.
- Biggs, D.S. 2010. 3D deconvolution microscopy. *Curr. Protoc. Cytom.* 12: 12.19.1–12.19.20.
- Byers, T.J., and D. Branton. 1985. Visualization of the protein associations in the erythrocyte membrane skeleton. *Proc. Natl. Acad. Sci. USA.* 82:6153–6157. <http://dx.doi.org/10.1073/pnas.82.18.6153>
- Das, A., C. Base, S. Dhulipala, and R.R. Dubreuil. 2006. Spectrin functions upstream of ankyrin in a spectrin cytoskeleton assembly pathway. *J. Cell Biol.* 175:325–335. <http://dx.doi.org/10.1083/jcb.200602095>
- Das, A., C. Base, D. Manna, W. Cho, and R.R. Dubreuil. 2008. Unexpected complexity in the mechanisms that target assembly of the spectrin cytoskeleton. *J. Biol. Chem.* 283:12643–12653. <http://dx.doi.org/10.1074/jbc.M800094200>
- Davis, L., K. Abdi, M. Machius, C. Brautigam, D.R. Tomchick, V. Bennett, and P. Michaely. 2009. Localization and structure of the ankyrin-binding site on  $\beta_2$ -spectrin. *J. Biol. Chem.* 284:6982–6987. <http://dx.doi.org/10.1074/jbc.M809245200>
- Di Paolo, G., and P. De Camilli. 2006. Phosphoinositides in cell regulation and membrane dynamics. *Nature.* 443:651–657. <http://dx.doi.org/10.1038/nature05185>
- Drisdell, R.C., J.K. Alexander, A. Sayeed, and W.N. Green. 2006. Assays of protein palmitoylation. *Methods.* 40:127–134. <http://dx.doi.org/10.1016/j.jymeth.2006.04.015>
- Fernández-Hernando, C., M. Fukata, P.N. Bernatchez, Y. Fukata, M.I. Lin, D.S. Bredt, and W.C. Sessa. 2006. Identification of Golgi-localized acyl transferases that palmitoylate and regulate endothelial nitric oxide synthase. *J. Cell Biol.* 174:369–377. <http://dx.doi.org/10.1083/jcb.200601051>
- Fukata, Y., and M. Fukata. 2010. Protein palmitoylation in neuronal development and synaptic plasticity. *Nat. Rev. Neurosci.* 11:161–175. <http://dx.doi.org/10.1038/nrn2788>
- Fukata, M., Y. Fukata, H. Adesnik, R.A. Nicoll, and D.S. Bredt. 2004. Identification of PSD-95 palmitoylating enzymes. *Neuron.* 44:987–996. <http://dx.doi.org/10.1016/j.neuron.2004.12.005>
- Fukata, Y., T. Iwanaga, and M. Fukata. 2006. Systematic screening for palmitoyl transferase activity of the DHHC protein family in mammalian cells. *Methods.* 40:177–182. <http://dx.doi.org/10.1016/j.jymeth.2006.05.015>
- Fukata, Y., A. Dimitrov, G. Boncompain, O. Vielemeyer, F. Perez, and M. Fukata. 2013. Local palmitoylation cycles define activity-regulated postsynaptic subdomains. *J. Cell Biol.* 202:145–161. <http://dx.doi.org/10.1083/jcb.201302071>
- Garbe, D.S., A. Das, R.R. Dubreuil, and G.J. Bashaw. 2007.  $\beta$ -Spectrin functions independently of Ankyrin to regulate the establishment and maintenance of axon connections in the *Drosophila* embryonic CNS. *Development.* 134:273–284. <http://dx.doi.org/10.1242/dev.02653>
- Gassama-Diagne, A., W. Yu, M. ter Beest, F. Martin-Belmonte, A. Kierbel, J. Engel, and K. Mostov. 2006. Phosphatidylinositol-3,4,5-trisphosphate regulates the formation of the basolateral plasma membrane in epithelial cells. *Nat. Cell Biol.* 8:963–970. <http://dx.doi.org/10.1038/ncb1461>
- Gomez, J.M., Y. Wang, and V. Riechmann. 2012. Tao controls epithelial morphogenesis by promoting Fasciclin 2 endocytosis. *J. Cell Biol.* 199:1131–1143. <http://dx.doi.org/10.1083/jcb.201207150>
- Greaves, J., and L.H. Chamberlain. 2011. Differential palmitoylation regulates intracellular patterning of SNAP25. *J. Cell Sci.* 124:1351–1360. <http://dx.doi.org/10.1242/jcs.079095>
- Hammond, G.R., M.J. Fischer, K.E. Anderson, J. Holdich, A. Koteci, T. Balla, and R.F. Irvine. 2012. PI4P and PI(4,5)P<sub>2</sub> are essential but independent lipid determinants of membrane identity. *Science.* 337:727–730. <http://dx.doi.org/10.1126/science.1222483>
- He, M., P. Jenkins, and V. Bennett. 2012. Cysteine 70 of ankyrin-G is S-palmitoylated and is required for function of ankyrin-G in membrane domain assembly. *J. Biol. Chem.* 287:43995–44005. <http://dx.doi.org/10.1074/jbc.M112.417501>
- He, M., W.C. Tseng, and V. Bennett. 2013. A single divergent exon inhibits ankyrin-B association with the plasma membrane. *J. Biol. Chem.* 288:14769–14779. <http://dx.doi.org/10.1074/jbc.M113.465328>
- Hoock, T.C., L.L. Peters, and S.E. Lux. 1997. Isoforms of ankyrin-3 that lack the NH<sub>2</sub>-terminal repeats associate with mouse macrophage lysosomes. *J. Cell Biol.* 136:1059–1070. <http://dx.doi.org/10.1083/jcb.136.5.1059>
- Hu, R.J., S. Moorthy, and V. Bennett. 1995. Expression of functional domains of  $\beta_6$ -spectrin disrupts epithelial morphology in cultured cells. *J. Cell Biol.* 128:1069–1080. <http://dx.doi.org/10.1083/jcb.128.6.1069>
- Hyvönen, M., M.J. Macias, M. Nilges, H. Oschkinat, M. Saraste, and M. Wilmanns. 1995. Structure of the binding site for inositol phosphates in a PH domain. *EMBO J.* 14:4676–4685.
- Ipsaro, J.J., and A. Mondragón. 2010. Structural basis for spectrin recognition by ankyrin. *Blood.* 115:4093–4101. <http://dx.doi.org/10.1182/blood-2009-11-255604>
- Ipsaro, J.J., L. Huang, and A. Mondragón. 2009. Structures of the spectrin-ankyrin interaction binding domains. *Blood.* 113:5385–5393. <http://dx.doi.org/10.1182/blood-2008-10-184358>
- Iwanaga, T., R. Tsutsumi, J. Noritake, Y. Fukata, and M. Fukata. 2009. Dynamic protein palmitoylation in cellular signaling. *Prog. Lipid Res.* 48:117–127. <http://dx.doi.org/10.1016/j.plipres.2009.02.001>
- Jenkins, P.M., C. Vasavda, J. Hostettler, J.Q. Davis, K. Abdi, and V. Bennett. 2013. E-cadherin polarity is determined by a multifunction motif mediating lateral membrane retention through ankyrin-G and apical-lateral transcytosis through clathrin. *J. Biol. Chem.* 288:14018–14031. <http://dx.doi.org/10.1074/jbc.M113.454439>
- Johnson, J.L., J.W. Erickson, and R.A. Cerione. 2012. C-terminal di-arginine motif of Cdc42 protein is essential for binding to phosphatidylinositol 4,5-bisphosphate-containing membranes and inducing cellular transformation. *J. Biol. Chem.* 287:5764–5774. <http://dx.doi.org/10.1074/jbc.M111.336487>
- Kizhatil, K., and V. Bennett. 2004. Lateral membrane biogenesis in human bronchial epithelial cells requires 190-kDa ankyrin-G. *J. Biol. Chem.* 279:16706–16714. <http://dx.doi.org/10.1074/jbc.M314296200>
- Kizhatil, K., J.Q. Davis, L. Davis, J. Hoffman, B.L. Hogan, and V. Bennett. 2007a. Ankyrin-G is a molecular partner of E-cadherin in epithelial cells and early embryos. *J. Biol. Chem.* 282:26552–26561. <http://dx.doi.org/10.1074/jbc.M703158200>
- Kizhatil, K., W. Yoon, P.J. Mohler, L.H. Davis, J.A. Hoffman, and V. Bennett. 2007b. Ankyrin-G and  $\beta^2$ -spectrin collaborate in biogenesis of lateral membrane of human bronchial epithelial cells. *J. Biol. Chem.* 282:2029–2037. <http://dx.doi.org/10.1074/jbc.M608921200>
- Li, Y., B.R. Martin, B.F. Cravatt, and S.L. Hofmann. 2012. DHHC5 protein palmitoylates flotillin-2 and is rapidly degraded on induction of neuronal differentiation in cultured cells. *J. Biol. Chem.* 287:523–530. <http://dx.doi.org/10.1074/jbc.M111.306183>
- Lingwood, D., and K. Simons. 2010. Lipid rafts as a membrane-organizing principle. *Science.* 327:46–50. <http://dx.doi.org/10.1126/science.1174621>
- Liu, S.C., L.H. Derick, and J. Palek. 1987. Visualization of the hexagonal lattice in the erythrocyte membrane skeleton. *J. Cell Biol.* 104:527–536. <http://dx.doi.org/10.1083/jcb.104.3.527>
- Martin, B.R., C. Wang, A. Adibekian, S.E. Tully, and B.F. Cravatt. 2012. Global profiling of dynamic protein palmitoylation. *Nat. Methods.* 9:84–89. <http://dx.doi.org/10.1038/nmeth.1769>
- Martin-Belmonte, F., A. Gassama, A. Datta, W. Yu, U. Rescher, V. Gerke, and K. Mostov. 2007. PTEN-mediated apical segregation of phosphoinositides controls epithelial morphogenesis through Cdc42. *Cell.* 128:383–397. <http://dx.doi.org/10.1016/j.cell.2006.11.051>
- Martinez-Palomou, A., I. Meza, G. Beaty, and M. Cerejido. 1980. Experimental modulation of occluding junctions in a cultured transporting epithelium. *J. Cell Biol.* 87:736–745. <http://dx.doi.org/10.1083/jcb.87.3.736>
- Mazock, G.H., A. Das, C. Base, and R.R. Dubreuil. 2010. Transgene rescue identifies an essential function for *Drosophila*  $\beta$  spectrin in the nervous system and a selective requirement for ankyrin-2-binding activity. *Mol. Biol. Cell.* 21:2860–2868. <http://dx.doi.org/10.1091/mbc.E10-03-0180>
- Nakatsu, F., J.M. Baskin, J. Chung, L.B. Tanner, G. Shui, S.Y. Lee, M. Pirruccello, M. Hao, N.T. Ingolia, M.R. Wenk, and P. De Camilli. 2012. PtdIns4P synthesis by PI4KIII $\alpha$  at the plasma membrane and its impact on plasma membrane identity. *J. Cell Biol.* 199:1003–1016. <http://dx.doi.org/10.1083/jcb.201206095>
- Nelson, W.J., R.W. Hammerton, A.Z. Wang, and E.M. Shore. 1990a. Involvement of the membrane-cytoskeleton in development of epithelial cell polarity. *Semin. Cell Biol.* 1:359–371.

- Nelson, W.J., E.M. Shore, A.Z. Wang, and R.W. Hammerton. 1990b. Identification of a membrane-cytoskeletal complex containing the cell adhesion molecule uvomorulin (E-cadherin), ankyrin, and fodrin in Madin-Darby canine kidney epithelial cells. *J. Cell Biol.* 110:349–357. <http://dx.doi.org/10.1083/jcb.110.2.349>
- Ohno, Y., A. Kihara, T. Sano, and Y. Igarashi. 2006. Intracellular localization and tissue-specific distribution of human and yeast DHHC cysteine-rich domain-containing proteins. *Biochim. Biophys. Acta.* 1761:474–483. <http://dx.doi.org/10.1016/j.bbali.2006.03.010>
- Peters, L.L., K.M. John, F.M. Lu, E.M. Eicher, A. Higgins, M. Yialamas, L.C. Turtzo, A.J. Otsuka, and S.E. Lux. 1995. Ank3 (epithelial ankyrin), a widely distributed new member of the ankyrin gene family and the major ankyrin in kidney, is expressed in alternatively spliced forms, including forms that lack the repeat domain. *J. Cell Biol.* 130:313–330. <http://dx.doi.org/10.1083/jcb.130.2.313>
- Rameh, L.E., A. Arvidsson, K.L. Carraway III, A.D. Couvillon, G. Rathbun, A. Crompton, B. VanRenterghem, M.P. Czech, K.S. Ravichandran, S.J. Burakoff, et al. 1997. A comparative analysis of the phosphoinositide binding specificity of pleckstrin homology domains. *J. Biol. Chem.* 272:22059–22066. <http://dx.doi.org/10.1074/jbc.272.35.22059>
- Razzini, G., A. Ingrosso, A. Brancaccio, S. Sciacchitano, D.L. Esposito, and M. Falasca. 2000. Different subcellular localization and phosphoinositides binding of insulin receptor substrate protein pleckstrin homology domains. *Mol. Endocrinol.* 14:823–836. <http://dx.doi.org/10.1210/mend.14.6.0486>
- Rocks, O., M. Gerauer, N. Vartak, S. Koch, Z.P. Huang, M. Pechlivanis, J. Kuhlmann, L. Brunsveld, A. Chandra, B. Ellinger, et al. 2010. The palmitoylation machinery is a spatially organizing system for peripheral membrane proteins. *Cell.* 141:458–471. <http://dx.doi.org/10.1016/j.cell.2010.04.007>
- Roth, A.F., Y. Feng, L. Chen, and N.G. Davis. 2002. The yeast DHHC cysteine-rich domain protein Akr1p is a palmitoyl transferase. *J. Cell Biol.* 159:23–28. <http://dx.doi.org/10.1083/jcb.200206120>
- Santangelo, P.J., A.W. Lifland, P. Curt, Y. Sasaki, G.J. Bassell, M.E. Lindquist, and J.E. Crowe Jr. 2009. Single molecule-sensitive probes for imaging RNA in live cells. *Nat. Methods.* 6:347–349. <http://dx.doi.org/10.1038/nmeth.1316>
- Shewan, A., D.J. Eastburn, and K. Mostov. 2011. Phosphoinositides in cell architecture. *Cold Spring Harb. Perspect. Biol.* 3:a004796. <http://dx.doi.org/10.1101/cshperspect.a004796>
- Sibarita, J.B. 2005. Deconvolution microscopy. *Adv. Biochem. Eng. Biotechnol.* 95:201–243.
- Simons, K., and M.J. Gerl. 2010. Revitalizing membrane rafts: new tools and insights. *Nat. Rev. Mol. Cell Biol.* 11:688–699. <http://dx.doi.org/10.1038/nrm2977>
- Thomas, G.M., T. Hayashi, S.L. Chiu, C.M. Chen, and R.L. Haganir. 2012. Palmitoylation by DHHC5/8 targets GRIP1 to dendritic endosomes to regulate AMPA-R trafficking. *Neuron.* 73:482–496. <http://dx.doi.org/10.1016/j.neuron.2011.11.021>
- Travé, G., A. Pastore, M. Hyvönen, and M. Saraste. 1995. The C-terminal domain of  $\alpha$ -spectrin is structurally related to calmodulin. *Eur. J. Biochem.* 227:35–42. <http://dx.doi.org/10.1111/j.1432-1033.1995.tb20357.x>
- Tsutsumi, R., Y. Fukata, J. Noritake, T. Iwanaga, F. Perez, and M. Fukata. 2009. Identification of G protein  $\alpha$  subunit-palmitoylating enzyme. *Mol. Cell Biol.* 29:435–447. <http://dx.doi.org/10.1128/MCB.01144-08>
- Wang, D.S., and G. Shaw. 1995. The association of the C-terminal region of  $\beta$ I $\Sigma$ II spectrin to brain membranes is mediated by a PH domain, does not require membrane proteins, and coincides with a inositol-1,4,5 triphosphate binding site. *Biochem. Biophys. Res. Commun.* 217:608–615. <http://dx.doi.org/10.1006/bbrc.1995.2818>
- Wang, D.S., R. Miller, R. Shaw, and G. Shaw. 1996. The pleckstrin homology domain of human  $\beta$ I $\Sigma$ II spectrin is targeted to the plasma membrane in vivo. *Biochem. Biophys. Res. Commun.* 225:420–426. <http://dx.doi.org/10.1006/bbrc.1996.1189>
- Wiederschain, D., S. Wee, L. Chen, A. Loo, G. Yang, A. Huang, Y. Chen, G. Caponigro, Y.M. Yao, C. Lengauer, et al. 2009. Single-vector inducible lentiviral RNAi system for oncology target validation. *Cell Cycle.* 8:498–504. <http://dx.doi.org/10.4161/cc.8.3.7701>
- Winkelman, J.C., F.F. Costa, B.L. Linzie, and B.G. Forget. 1990.  $\beta$  spectrin in human skeletal muscle. Tissue-specific differential processing of 3'  $\beta$  spectrin pre-mRNA generates a  $\beta$  spectrin isoform with a unique carboxyl terminus. *J. Biol. Chem.* 265:20449–20454.